Cluster isolated chemical reactions

J. M. Mestdagh; M. A. Gaveau; C. Gee; O. Sublemontier; J. P. Visticot

PLEASE SCROLL DOWN FOR ARTICLE

Cluster isolated chemical reactions

by J. M. MESTDAGH, M. A. GAVEAU, C. GÉE, O. SUBLEMONTIER
and J. P. VISTICOT

Commissariat à l'Energie Atomique, DSM, DRECAM, SPAM, Bâtiment 522,
Centre d'Etude, Saclay, F-91191 Gif-sur-Yvette Cedex, France

The study of chemical reactions in clusters is a rapidly growing field that is attractive for investigating medium effects in reaction dynamics. Cluster isolated chemical reaction (CICR) is a new direction developed in our laboratory, which enables quantitative studies to be made in that field. CICR experiments consist in depositing a controlled number of reactants on large van der Waals clusters that play the role of a solvent of fairly well known size, structure and temperature. This offers enormous advantages, both on the experimental side and for further theoretical investigations. The present review intends to draw together informations that are pertinent for developing experiments and concepts towards understanding chemical reactions in clusters, through CICR-type experiments. In particular, it reviews the questions first of generating and controlling the properties of large van der Waals clusters and secondly of attaching reactants to clusters and controlling their number and location in the cluster. Besides reviewing thoroughly the CICR work done so far in our laboratory, the present paper also reviews part of the vast literature pertaining to reaction dynamics in large van der Waals clusters.

1. Introduction

Much of the attention of the reaction dynamics community has been drawn towards detailed understanding of the mechanism of chemical reactions in the gas phase. Particular emphasis was given to reactions occurring under the single collision regime. The achievement of crossed-molecular-beam machines since the late 1960s allowed very detailed studies pursuing the goal of state-to-state chemistry. The book by Levine and Bernstein [1] contains a comprehensive review of what is going on in the field. In particular it outlines the constant interplay between theory and experiment and makes clear that developing both fancy quantum treatments and intuitive models helps us tremendously to understand the elementary mechanisms of chemical reactions. Studies of the $F + H_2$ system and their isotop analogues reveal the direction in which the field is going at present. This system is a benchmark test of quantum-chemical methods [2, 3] and tends to replace the simpler and now well understood $H + H_2$ system [4].

Although solution chemistry is one of the oldest areas in physical chemistry, it has begun to be understood from the molecular point of view only less than 20 years ago. Two recent review papers have highlighted the field [5, 6].

Clusters constitute now well established bridges between gas-phase and condensed-phase phenomena [7–12]. An outstanding example is the use of clusters to unravel size effects in the transition from van der Waals to metallic bonding [13]. Of course, clusters can also be used in reaction dynamics for *bridging the gap* between gas phase and condensed phase or solution chemistry. In this context, clusters of solvent molecules to which reactant molecules are attached offer a potentially convenient and powerful way of connecting the reaction dynamics of the reactant pair, free of external perturbations to that of the solvated pair. The size of the solvent cluster just needs to

be varied from very small (ultimately a van der Waals molecule of only the two reactants with no solvent molecule present) to very large clusters where many solvent molecules are present. Several collections and review papers have highlighted the role of cluster studies as useful steps to unravel the complex behaviour of reactants in liquid or solid solvents [14–17]. Recent studies of the 1-naphthol $(H_2O)_n$, $(NH_3)_n$, $\cdots$ systems well exemplifies the point. The proton transfer reaction that is promoted by laser excitation in these systems has been followed from $n = 1$ to many hundreds both by resonant two photon ionization spectroscopy [18] and in real-time measurements [19]. This provides a step towards a unified picture of the dynamics of proton transfer reactions in solvents.

1.1. *Scope of the review*

Our laboratory has initiated work along the idea of using large clusters of solvent atoms or molecules to unravel the effect of a surrounding on the dynamics of reactants deposited on the cluster. An *ideal experiment* in that field would be to dispose of a medium of known size, structure and internal energy, with a knowledge of interaction energies between the solute and the solvent. The need for such *ideal experiments* is made very acute by recent theoretical developments that open the route to modelling accurately fundamental aspects of reaction dynamics in solution [6] and in clusters [16 a, b].

Although chemical reaction in clusters is a fairly new research field, it has already motivated an impressive number of publications. We therefore limit the scope of this review to the literature that is pertinent to approaching experimentally the above definition of an *ideal experiment*, with the further limitation that *only large neutral clusters* are considered here.

(1) Section 2 reviews the way of generating and characterizing large homogeneous clusters of atomic and molecular solvents bound by van der Waals forces or by hydrogen bonds. The structure and thermodynamics of these clusters are also reviews in this section. The optical spectroscopy of these clusters is beyond the scope of the present review. It essentially deals with the transition from atomic Rydberg states to solid-state excitons as the cluster size is increased. Such work has been exemplified in [20]

(2) The attachment of guest atoms or molecules to host clusters is reviewed in section 3. Experimental considerations are addressed together with spectroscopic properties of the reactants attached to clusters.

(3) Reaction dynamics in clusters is the topic of section 4. Emphasis is placed on experimental studies, but theoretical aspects will also be referred whenever appropriate.

(4) Finally, the method for monitoring the *cluster isolated chemical reaction* (CICR) that was developed in our laboratory is detailed in section 5 together with the main results that have been obtained so far using this technique in our laboratory. This will allow us to make a step towards answering the main question that motivates our work: to what extent does the reaction medium affect reaction dynamics? The CICR method is partly based on the strict control of reactant deposition on clusters. For this reason, much attention is given to the attachment of reactants to clusters in section 3, and especially to the way of determining the average number of reactants that has been deposited per cluster.

1.2. *Related topics*

Several important topics are not discussed here although they have strong connections with the present review.

(1) Photoinduced reactions in 1:1 van der Waals complexes. The study of such processes was pioneered in two groups by Wittig and co-workers [21] and by Jouvet and co-workers [22–24]. Both experimental work and theoretical work along this line have been reviewed recently [16a, 21–24].

(2) Photoinduced electron and proton transfer reactions in clusters formed with one chromophore attached to a few solvent molecules (often less than 10). Several examples have been reviewed in [25]. An extensive study of the twisted intramolecular charged transfer emission of 4-N,N-dimethylaminobenzoate solvated by water molecules exemplifies the field [26], as well as the studies quoted above concerning proton transfer reactions in the 1-naphthol $(H_2O)_n$, $(NH_3)_n$, $\cdots$ systems [18, 19]. Other excited-state proton transfer reactions have also been studied recently in the time domain [27, 28].

(3) Cage effects in matrices. Only very limited reference has been made to this important field. An important review of new developments in matrix isolation spectroscopy has appeared recently [29].

(4) Cage effect in the $I_2^-(CO_2)_n$ and $Br_2^-(CO_2)_n$ ionic systems for $n \leqslant 24$. These systems were studied by Lineberger's group [30–33].

(5) Ion–molecule reactions within cluster ions is a very developed field that has been reviewed recently by Castleman [34]. Several chapters of the book by Haberland [10] cover this question also.

(6) Photoinduced chemical reactions on insulator and metal surfaces [35–37].

The present review does not cover systematically studies involving quantum clusters (helium and H_2 clusters). These clusters are indeed fluids and require studies that address the question of superfluidity in finite systems [38]. Such studies are far from the scope of the present review. However, reference is made in section 3 to studies that are more closely related to the present topic: spectroscopy of guest molecules deposited on clusters, and association reaction between guest molecules.

Instead of being the medium where the reaction dynamics takes place, van der Waals or hydrogen-bonded clusters may also be collision partners in their own, and their collision dynamics has been investigated. Essentially three directions are explored that are not reviewed here thoroughly.

(1) Momentum transfer in a scattering experiment of atoms with clusters allows one to size select the clusters. Intracluster dynamics and scattering dynamics of size selected clusters can thus be investigated. The groups of Buck, Huisken and Toennies are active along this line. Part of the studies performed in these groups provide information directly relevant to the present review and appear below. The other work performed recently in the same groups concern infrared spectroscopy of clusters [39–48], inelastic scattering [49–52], and electron impact ionization and fragmentation of size-selected clusters [53, 54]. They are not reviewed here.

(2) Scattering of large argon clusters (approximately Ar_{1000}) on graphite surfaces is currently under investigation by Pradère's group [55–57], a topic that was pioneered by Gspann and Krieg [58]. The question of cluster–surface collisions has several implications in the field of collision-activated reactions when high-velocity clusters collide with hard surfaces. The localized heating that follows

the cluster–surface collision indeed opens up the possibility of inducing reactions between reactants that are embedded in the cluster [59]. Under these extreme conditions, reactions that have a very high activation barrier can even be observed. The corresponding chemistry motivates extensive theoretical investigations on the ground of molecular dynamics calculations [60–64].

(3) Reactions of barium atoms with both small and large molecular clusters of N_2O, NO_2, SO_2 and H_2O has been investigated [65–68]. It was found that the branching ratio to chemiluminescence is zero in large-cluster reactions [67, 68]. Moreover, non-chemiluminescent products are substantially colder, rotationally and vibrationally in the cluster reaction than in the gas phase [66]. The reactivity of oxygen atoms with small van der Waals clusters has been investigated systematically by Naaman's group [69–78]. Among many interesting results it was found that the formation of OH, that is the formation of the gas-phase product is inhibited in the reaction of oxygen with cyclohexane clusters, whereas, the *solution-like* product, cyclohexanol, is formed [73]. This example demonstrates, if needed, the transition from gas phase to solution reaction dynamics by using clusters to bridge the gap between both phases.

2. Formation and properties of large host clusters

An extensive account of the experimental methods used to generate and characterize cluster beams has been given in the two books edited by Haberland [10, 11], and in the work of Kappes and Leutwyler [79]. The books edited by Haberland also provide very extensive information about cluster properties. Further information, both experimental and theoretical, can be found in [80].

The present section gives a rapid overview of the field with special emphasis on large clusters bound by weak forces that are used in our laboratory as reaction media: argon clusters essentially, and a few molecular clusters.

2.1. *Experiment*
2.1.1. *Cluster formation in supersonic expansions*

Beams of van der Waals clusters are produced by a supersonic expansion of a gas into vacuum through a nozzle of small diameter [81, 82]. Briefly, the supersonic expansion is associated with a sudden drop in both the pressure and the temperature of the expanding gas. This results in condensation when the expanding gas reaches and crosses the conditions of gas–liquid or gas–solid equilibrium. The nucleation process that is active under these conditions is extremely complex. It is quite far from being totally understood, mainly because of the rapidity of the pressure and temperature changes: two to six orders of magnitude in a few microseconds. An account of nucleation theories has been provided in [79].

Hagena [83] has determined a scaling law that allows one to compare different expansion conditions of the same gas using a single parameter Γ given by

$$\Gamma = n_0 \, d^{\,q} T_0^{[(2-\gamma)\,q-2]/2(\gamma-1)}, \tag{1}$$

where γ is the ratio C_P/C_V of the heat capacities of the gas, n_0 and T_0 are the gas number density and temperature respectively under the stagnation conditions, d is the nozzle diameter and q is an empirical parameter that depends on the gas. It ranges between 0·5 and 1 ($q = 0·85$ for argon [84]). Different expansion conditions associated with the same scaling parameter Γ have the same cluster composition. Hagena introduced a further parameter that allows one to compare different gases. He defined a species

characteristic temperature T_{ch} and radius r_{ch} and transformed the gas-dependent scaling parameter Γ into a dimensionless parameter Γ^* that is gas independent [85]. Γ^* has the expression

$$\Gamma^* = nr_{ch}^3 \left(\frac{d}{r_{ch}}\right)^q \left(\frac{T_0}{T_{ch}}\right)^{[(2-\gamma)q-2]/2(\gamma-1)}. \qquad (2)$$

The sublimation enthalpy (ΔH_0) at 0 K, the atomic mass m and the density ρ of the solid define the characteristic quantities T_{ch} and r_{ch} of the species under consideration according to

$$r_{ch} = \left(\frac{m}{\rho}\right)^{1/3}, \qquad (3)$$

$$T_{ch} = \frac{\Delta H_0}{k}$$

where k is the Boltzmann constant. The scaling parameter Γ^* allows one to distinguish between different regimes [85]:

$\Gamma^* < 200,$ no cluster formation,

$200 < \Gamma^* < 1000,$ small-cluster regime, clusters of less than 100 monomers,

$\Gamma^* > 1000,$ large-cluster regime, clusters of more than 100 monomers.

2.1.2. *Size of clusters*

Several methods have been developed to measure the mean size and the size distribution of clusters in cluster beams. Mass spectrometry is certainly the simplest of these methods. Unfortunately, it is potentially very inaccurate because neutral clusters need to be ionized before being mass analysed [79]. The ionization step usually results in phenomena such as cluster ion fragmentation, multiple ionization and mass-sensitive yield of ion detectors that bias severely measured mass distributions. Three types of method that do not require ionization of the neutral are preferred.

(1) *Electron diffraction*. The shape of the Debye–Scherrer rings in electron–cluster diffraction experiments contain information about the mean size of the clusters [86]. The method has been applied for determining the mean size of clusters in supersonic expansions of argon [87], CO_2 [88] and SF_6 [89].

(2) *Photon scattering*. The cross-section for Rayleigh scattering varies as the square of the cluster size. This provides an easy-to-perform, sensitive and non-destructive technique to determine relative mean quadratic size of clusters in beams formed under different conditions [90]. However, the absolute de-termination of mean sizes seems difficult with this method.

(3) *Atom scattering*. Although it is not easy to handle, this method is the most widely used at the moment. Clusters are collided with atoms and the momentum transfer resulting in the collision is measured. The method has several variants depending on the way of measuring the momentum transfer.

The atom scattering method was first applied by Gspann and Vollmar [91] to deflect nitrogen clusters by an intense secondary beam under the multicollision regime, the heavy clusters being less deflected than the light clusters. The size distribution of the clusters was found to be given by a log-normal probability function.

Buck and Meyer [92, 93] used a crossed-molecular-beam apparatus to monitor both the laboratory scattering angle and the laboratory velocity of helium atoms elastically scattered by molecular clusters in the single-collision regime. Taking

advantage of the kinematics of the helium–cluster collisions these workers have selected individual clusters of small sizes ($n \leqslant 10$). A full account of the method has been given in [94]. More recently, the same group has analysed diffraction oscillations in the angular distribution of helium atoms in the same experiment. Comparison of the observed oscillations to model calculations yield information about the mean size $\bar{n}$ and the size distribution of the cluster [95]. The width of the latter is $\bar{n}/2$ and $\bar{n}$ is well reproduced by the formula

$$\bar{n} = 38 \cdot 4 \left(\frac{\Gamma^*}{1000} \right)^{1 \cdot 64} \text{ for } 6 < \bar{n} < 90, \tag{4}$$

in terms of the Γ^* parameter defined in equation (2).

The group of Toennies and co-workers [96] has recently performed a small-angle ($\theta < 20$ mrad) scattering experiment under the single-collision regime to determine the size distribution of large helium clusters ($\bar{n} = 10^3$–10^4) [96]. Here again a broad log-normal distribution was found.

Instead of observing deflections in a crossed-beam apparatus, it is also possible to monitor the collisional momentum transfer in a beam–gas experiment. This was achieved both by our group by measuring the velocity change of clusters as they experience collisions with a buffer gas [97], and by Châtelet and co-workers [98] by measuring the broadening of the cluster beam. Both experiments yield comparable results for argon clusters, in agreement with the size determination performed by electron diffraction [87]. These values are a factor of about three larger than those provided by equation (4). Strikingly, these large average sizes have been measured for clusters generated using Campargue [81] sources whereas the other measurements correspond to Fenn-type sources [82].

2.2. *Properties of large homogeneous clusters*
2.2.1. *Structure and phase of clusters*

Much of the present knowledge about structure of large van der Waals clusters was obtained by electron diffraction experiments. A full account of the method has been given by Torchet [86]. Two reviews are also available [99, 100].

Argon clusters have an icosahedral structure up to about 800 atoms. When they contain more than 10000 atoms, they have a crystalline fcc structure of solid argon in the bulk [87, 101–104]. The transition region between 1000 and 10000 atoms, that is the transition region between icosahedral and crystalline structures is still a controversial subject. Several theoretical models have been proposed that confirm the stability of the icosahedral structure in small clusters and that of the fcc form in large clusters [105]. A very recent atomic-scale growth model for van der Waals crystals has been used to account quantitatively for the electron diffraction patterns in $Ar_{\bar{n}=3000}$ clusters [106]. The model shows that kinetic effects dominate the nucleation, and that the structure of the growing crystal is not necessarily that of the lowest energy in the infinite crystal. A crucial role is played in the model by particles with a fivefold symmetry as in decahedra and icosahedra.

Methane and nitrogen behave very much like rare gases. Large clusters formed with several thousands of these molecules have a crystalline structure with the molecular centres at fcc lattice sites whereas very small clusters have a polyicosahedral structure [107, 108]. Although SF_6 is another spherical molecule, it behaves differently from argon since a cluster as small as 100 molecules already has the structure of the

bulk material [109]. The same observation was done for CO_2 [88, 108]. SF_6 clusters deserve extensive investigations, both experimentally and theoretically and these revealed the existence of a transition between a monoclinic structure at low temperatures and a bcc structure at high temperatures [89, 110, 111]. Water clusters are very different. The small clusters are amorphous solids whereas the large clusters have a diamond cubic structure, that is they are a metastable phase of bulk ice [112]. The different behaviour of water might be related to the bonding between water molecules that goes through a network of hydrogen bonds.

A rule of thumb can be stated. Very large solid clusters, whatever their nature, show a crystalline structure that is known in the bulk solid. The structure of small clusters is more contrasting; either it is identical with the structure of large clusters (CO_2 and SF_6) or it is icosahedral (rare gases, CH_4 and N_2), or it is disordered (H_2O).

Clusters are not necessarily solid. Helium clusters are liquid because of the quantum character of condensed helium. The first evidence for superfluidity in a finite-sized helium droplet has even been provided recently by the Toennies' group in Göttingen [38].

Liquid molecular clusters have been reported for many molecules such as BCl_3, Cs_2, CCl_4 and many organic molecules. Several tens of molecules have been investigated by Bartell's group using electron diffraction. This has provided good knowledge of those substances that lead to liquid-like clusters and of those that lead to crystalline structures [100, 113]. These investigations aimed to unravel that complex nature of one of the simplest transformations of matter, that of freezing. The general idea of these experiments was to generate large liquid clusters in a supersonic expansion and to monitor by electron diffraction the freezing process that results in evaporative cooling of the cluster [113–117]. One of the outcomes of this research is the construction of a dimensionless index R_c for deciding whether clusters generated in supersonic expansions are solid or liquid [113]. The empirical criterion for clusters to be liquid is

$$R_c = \frac{T_b - T_m}{T_b} + 0.007 \left(\frac{\Delta S_m}{R}\right)^2 < 0.32, \tag{5}$$

where R is the gas constant. T_b and T_m are the normal boiling and freezing points respectively of the substance under consideration, and ΔS_m is its molar entropy of fusion. This equation has been tested on more than 50 different substances. It has been revisited recently for interpretation on the basis of current nucleation theories [118].

2.2.2. *Temperature of clusters*

The experimental determination of cluster temperatures is made by two routes.

(1) One is to detect directly the thermal motion of the particles forming the clusters. This was achieved in the electron diffraction experiments [86]. The shape of Debye–Scherrer rings contains information on this thermal motion in addition to information on size and structure that has been reviewed above [119]. The temperatures found by this technique in the expansion of pure gases (no seeding gas) are 27 ± 3 K for $Ar_{<50}$ [103], 32 ± 2 K for $Ar_{50 < n < 750}$ [87], 108 ± 10 K for $(CO_2)_{\approx 8000}$ [112] and 180 ± 20 K for $(H_2O)_{<200}$ [112].

(2) The other route is to deposit a molecule into the cluster and to measure its rotationally or vibrationally resolved infrared spectrum. For example, SF_6 deposited inside clusters of approximately 4000 helium atoms have been used to measure a temperature of 0.37 ± 0.05 K for the helium cluster [120].

Having statistical thermodynamics in mind, one may think of clusters in terms of either the canonical or the microcanonical ensembles. We are thus thinking either about their temperature or their internal energy. Unfortunately, the way that clusters are generated in supersonic expansions never provides clusters with a well defined temperature or internal energy. The evaporative ensemble, first anticipated by Gspann [121], and developed as a theory by Klots [122–127] is the current way to bypass this difficulty, and to model the evolution of ill-defined isolated clusters. The major result of the theory is that cluster temperatures can be determined accurately even without knowing exactly the initial state of the clusters, just after they have been formed. The basic assumption in Klots' theory is that the cluster has evaporated at least one particle between the time at which it has been formed and the time at which the observation is performed (tens of microseconds in practice). Particle evaporation is the only term of energy loss included in the model. In particular, collisions and radiative cooling processes are neglected. The evaporative ensemble theory has helped one to derive a phenomenological relation that relates the final temperature T_{cl} of the cluster to the molar heat of evaporation ΔH_0 at 0 K [122]:

$$T_{cl} \approx \frac{1}{\gamma} \frac{\Delta H_0}{R}, \tag{6}$$

where R is the gas constant. The Gspann dimensionless parameter γ is nearly independent of the size and nature of the cluster. It is equal to about 25 for typical laboratory observation time scales of tens of microseconds [124, 125]. Although the theory of Klots is widely accepted, it has been revisited several times in the recent literature [128, 129].

It must be noted that cluster temperatures can be decreased appreciably below T_{cl} by heat exchange with a coexpanding carrier gas. This possibility has been demonstrated several times in the past [130, 131]. It has been used recently to vary systematically the temperature of SF_6 cluster in order to explore solid-phase transitions of the cluster [89]. The phase transition in clusters is indeed an important issue for those groups involved in modelling clusters by molecular dynamics or by Monte Carlo calculations. The corresponding literature is impressive and is impossible to review within the format of the present paper.

3.   Large host clusters with guest atoms or molecules
3.1. *Experiment*
3.1.1. *The pick-up technique*

The pick-up technique is an elegant and efficient technique to deposit guest atoms or molecules on large host clusters. It was developed 10 years ago by Scoles and co-workers [132]. The supersonic expansion of the host cluster is crossed by a beam of the guest particles just in front of the skimmer that extracts the beam. Collisions between the host clusters and the guest particles result in the trapping of the guest particles by the clusters.

This technique is now used by several groups. Toennies and co-workers [133] have used it to attach foreign atoms to helium clusters. It has also been used by Huisken and Stemmler [134] for work along the lines initiated by Scoles and co-workers. Hertel and co-workers [133, 136] have adapted the technique to clusters generated in a pulsed expansion. They attached sodium atoms to water and to ammonia clusters. Finally, the pick-up technique has been used in our laboratory to deposit reactants on large

clusters produced in a Campargue [81] source. Since the silence zone between the nozzle and the skimmer of such a source can hardly be penetrated by a foreign gas, we performed the pick-up after the skimmer. The cluster beam is passed through a vapour of the guest particles, either coming from a secondary beam or more simply being a buffer gas.

The pick-up technique has deserved molecular dynamics simulations [137–139]. The capture cross-section is close to the geometrical size of the cluster when the mass of the guest particle is comparable with or larger than the mass of the monomers forming the host cluster [138]. In contrast, very light particles such as helium atoms colliding with argon clusters are scattered and are not captured. This point is confirmed by extensive elastic and inelastic scattering studies of helium atoms by large argon clusters by Buck and co-workers [50, 51]. The purpose of these very novel and elegant experiments was to inform about the vibrational spectrum of free clusters.

3.1.2. *Average number of reactants per clusters*

Emphasis is given in this section to determining the average number of reactant deposited per cluster by the pick-up technique. We shall see in section 5 that such knowledge is the key that makes the CICR method developed in our laboratory quantitative.

The pick-up technique that is used to deposit guest particles on large clusters is a random process with no memory between successive collisions. It thus follows Poisson statistics apply. Let $\langle m \rangle$ be the average number of guest particles picked up per cluster. According to the Poisson statistics, the probability $P_q(\langle m \rangle)$ of finding a cluster that carry q guest particles is

$$P_q(\langle m \rangle) = \frac{\langle m \rangle^q}{q!} \exp(-\langle m \rangle). \tag{7}$$

The above expression has only one parameter $\langle m \rangle$. Therefore knowledge of $\langle m \rangle$ is enough to characterize fully the distribution of the number of guest particles deposited per cluster. Several techniques have been developed in our laboratory to determine the average number $\langle m \rangle$ experimentally.

3.1.2.1. *The relative flux method.* The cluster beam (host cluster + guest particles) is

scattered into a chamber (the compression chamber) that is pumped through a small conductance. Doing this results in the destruction of the clusters and the composition of the gas in the compression chamber reflects the composition of the clusters. A mass spectrometer is used to perform the gas analysis in the compression chamber. Two different arrangements have been used. In the first, the compression chamber is large enough to contain the mass spectrometer that is thus used to measure the partial pressures p_{guest} and p_{host} of both gases in the chamber. This is achieved after proper calibration of the mass spectrometer by filling the chamber with pure gases and using an absolute pressure gauge (a viscosity gauge for example). Let $\bar{n}$ be the mean size of the clusters as determined by one of the methods described in section 2.1.2. Let $\langle m \rangle$ be the desired mean number of guest particles per cluster. It is deduced from the partial pressure measurement according to [140]:

$$\langle m \rangle = \bar{n} \frac{p_{guest}}{p_{host}} \frac{M_{host}^{1/2}}{M_{guest}^{1/2}}, \tag{8}$$

where M_{guest} and M_{host} are the masses of the guest and host particles respectively. The

coefficients $M_{\mathrm{host}}^{1/2}$ and $M_{\mathrm{guest}}^{1/2}$ in the above expression reflect the inverse proportion of partial pressures inside the compression chamber and conductance of the chamber aperture for the specified gas.

The second arrangement uses a small glass cell as compression chamber with the mass spectrometer installed outside the cell, close to its outlet. In that case, the quantity $\langle m \rangle$ is deduced from the readings i_{host} and i_{guest} of the mass spectrometer according to

$$\langle m \rangle = \bar{n}\frac{i_{\mathrm{guest}}}{i_{\mathrm{host}}}. \qquad (9)$$

Several complications arise when performing this measurement. The cluster beam can also carry monomers, the fraction of which must be determined. This is achieved in our experiment as shown in [141]. The other complications mainly result from the necessity to measure accurately small partial pressures of the guest molecule. For instance, outgas from the walls of the compression chamber can cause serious difficulties. The second arrangement is less sensitive to this trouble.

3.1.2.2. *The decay flux method.* The flux at the centre of the cluster beam is monitored with the pick-up gas both present and absent in the pick-up region. The collisions between the host clusters and the guest particles in the pick-up zone result in a broadening of the cluster beam because of momentum conservation, and therefore the beam flux at the centre of the beam is attenuated in proportion with

$$\frac{\langle m \rangle}{\bar{n}}\frac{M_{\mathrm{guest}}}{M_{\mathrm{host}}}, \qquad (10)$$

thus allowing determination of $\langle m \rangle$ [142]. The method is very similar to that developed in [98] for determining the mean size of the clusters.

3.1.2.3. *Laser-induced fluorescence.* This method is the simplest to use when the guest particle can be probed by laser-induced fluorescence. We have applied this method to determine the average number of barium atoms that have been deposited on large argon clusters. We found indeed that laser light near 540 nm wavelength hits the resonance transition of a single barium atom solvated on an argon cluster and therefore induces fluorescence of excited barium. On the other hand, clusters containing more than one barium atom lead to the formation of barium subclusters that have a different absorption band [143]. The laser-induced fluorescence signal associated with the absorption of a single barium atom per cluster thus follows the Poisson distribution $P_1(\langle m_{\mathrm{Ba}} \rangle)$ when varying the as yet unknown mean number $\langle m_{\mathrm{Ba}} \rangle$ of barium atom per cluster. The range of variation of $\langle m_{\mathrm{Ba}} \rangle$ must contain $\langle m_{\mathrm{Ba}} \rangle = 1$ which corresponds to the maximum of $P_1(\langle m_{\mathrm{Ba}} \rangle)$. Then it is easy to relate the variation in the laser-induced fluorescence signal to the known variation of the Poisson distribution $P_1(\langle m_{\mathrm{Ba}} \rangle)$, thus determining the scale of variation of $\langle m_{\mathrm{Ba}} \rangle$ [144].

3.2. *Spectroscopy of guest molecules deposited on clusters*

The present section does not attempt to review thoroughly the vast literature concerning the spectroscopy of guest atoms or molecules embedded in host clusters. It focuses on some properties of the guest–host system that are important for further investigation of reaction dynamics in large cluster environments.

The distinction between small and large host clusters is especially acute in this section. Guest–host systems with small host clusters are dominated by the existence of

several isomers, and by size-specific phenomena such as magic numbers and shell closure. Guest and host behaviours can hardly be dissociated in these systems. Such situations are exemplified by the microsolvation of aromatic molecules in rare gases [12, 145–150]. Further bibliographic information can be found in [151] for organic molecules solvated by a few hydrogen-bonding molecules. In contrast, large host clusters lead to smooth size effects. Relevant questions in this case are the location of the guest particle, the energy exchange between guest and host, the mobility of the guest particle on (or in) the host cluster and the association between several guest particles on (or in) the same host. Most of these questions go beyond sole spectroscopic motivations. They give insight into photochemistry and are therefore reviewed in section 4.

3.2.1. *Probing the location of the guest atom or molecule*

Deposition of SF_6 molecules in large argon clusters is the first example where the pick-up technique was used with the hope of depositing molecules at the surface of the host cluster rather than having it solvated in the interior of the cluster [132]. This was checked by the infrared spectroscopy of the SF_6 guest.

Systematic studies have been done by Scoles' group to determine the fate of the picked-up molecules: surface as against interior solvation. For instance, SiF_4 is at the surface of argon clusters of all sizes, whatever the method used to deposit the molecule on clusters (pick-up or coexpansion). In contrast, SF_6 stays at the surface of the cluster only for sufficiently large clusters and pick-up deposition of the molecule [152]. These results plus others concerning different guest molecules [153, 154] have been rationalized on the basis of classical molecular dynamics calculations [155]. The parameters σ and ε defining the Lennard-Jones potentials used in the calculation for both Ar–Ar and guest–Ar interactions have served to construct two dimensionless parameters:

$$\sigma^* = \frac{\sigma(\text{guest} - \text{Ar})}{\sigma(\text{Ar} - \text{Ar})}, \quad \varepsilon^* = \frac{\varepsilon(\text{guest} - \text{Ar})}{\varepsilon(\text{Ar} - \text{Ar})}. \quad (11)$$

Large ε^* and small σ^* are associated with interior solvation whereas small ε^* and large σ^* lead to surface solvation.

Probing the surface or the interior location of host particles has also been done by visible spectroscopy. For example, surface location of barium atoms on argon host clusters has been revealed in our laboratory by observing the splitting of the barium resonance line into two bands when barium is deposited in large argon clusters [156, 157]. As above, classical molecular dynamics simulations are a useful complement to the experiment and give a consistent picture of the solvation of the guest atom by the host cluster. These calculations have modelled the effect of the argon surroundings on the barium spectroscopy by vector addition of pairwise potentials describing the $Ba(^1S_0$ and $^1P_1)$–Ar and Ar–Ar interactions. A similar model where energy levels of the guest atom are treated as perturbed atomic states has been used by Möller and co-workers [158] when assigning electronic excitation bands in $Xe(Ar)_n$ and $(Xe)_m(Ar)_n$ clusters near electronic transitions of pure xenon.

3.2.2. *Guest molecule spectroscopy as a probe of host properties*

Infrared spectroscopy of the guest molecule has been used to go beyond simple location analysis of the guest in the host. It has also been used to obtain information on the guest–host interaction, and more precisely on the dynamical state of the host

cluster. This has been exemplified by Scoles and co-workers [159] when studying $SF_6(Ar)_n$, $SF_6(Kr)_n$ and $SF_6(Xe)_n$ with n ranging between 100 and 10000. Changes in the infrared spectra between small and large clusters have been attributed to the transition of clusters from the icosahedral structure, known to be the most stable for small clusters, to the fcc structure which is observed in the bulk. High-resolution infrared spectroscopy of SF_6 molecules has also been to measure the temperature of liquid-helium clusters [160].

4.   Photochemistry of guest atoms or molecules in clusters

Studies devoted to the reaction dynamics of guest molecules on (or in) large host clusters are rather rare. Most of the attention has indeed been drawn towards small systems, essentially because two goals were followed: firstly the dynamics of bimolecular reactions were elucidated by limiting the phase space that is accessible to the system, which motivates for studies using 1:1 van der Waals complexes of the two reactants; secondly the role of the first solvent shell in solvent-induced chemical reactions such as electron-transfer reactions, was elucidated.

Studying reaction dynamics in large clusters has different motivations that have already been encountered above when considering the spectroscopy of a guest particle in host clusters. Large host clusters is the domain of smooth size effects. The role of the host cluster is considered in terms of a solvent cage or of a reaction medium with a possible *chaperon* effect. The *chaperon* effect directly addresses the important issue of the exchange of energy between the reactive system and the host cluster. Another issue is the fate of the reaction products. Do they evaporate off the cluster, or do they stay solvated and further exchange energy with the cluster?

Different classes of chemical reactions have been studied so far with the above questions in mind:

(1) photodesorption of a single guest atom off the host cluster, which is exemplified in the next section by reviewing a series of studies, partly done in our laboratory, on photoexcitation and photodesorption of barium atoms off $BaAr_n$ clusters;

(2) photodissociation of the guest molecule;

(3) association reactions between two or more guest atoms or molecules;

(4) very exoergic reactions between guest reactants, which has been developed in our laboratory; the CICR technique has been developed for that purpose and is reported separately in section 5.

4.1. *Photodesorption of barium off $BaAr_n$ clusters*
4.1.1. *Excitation of barium fluorescence in argon clusters*

The photoexcitation spectrum of $Ba-Ar_{\approx 1000}$ clusters has been measured in our laboratory, together with the resulting fluorescence emission. The excitation spectrum is split into two bands, one on each side of the resonance transition $^1S_0 \rightarrow {}^1P_1$ of free barium. As already reported in section 3.2.1, this is due to surface location of barium. The blue and red bands can be assigned respectively to Σ- and Π-like states of a $Ba-Ar_n$ pseudo-diatomic molecule [156, 157].

4.1.2. *Competition between two decay channels*

The Π-like state has only one luminescent decay channel. It corresponds to the emission of barium atoms that stay attached to the cluster. The emitting atoms can be considered as relaxed into the well of the Π-like state. In contrast, the Σ-like state has

two different luminescent decay channels. One is the same as that encountered when photoexciting the Π-like state. Again, it corresponds to barium emitting from the cluster after relaxation into the potential well of the Π-like state. The other luminescent channel corresponds to photodesorption of excited Ba ($6s6p\ ^1P_1$) atom off the cluster followed by radiative decay of barium as a free atom. Photoexcitation of the Σ-like component thus leads to an interesting competition between desorption and relaxation. It has been investigated in detail in our laboratory.

The degree of polarization of the fluorescence light emitted from both decay channels has been investigated as a function of the polarization of the laser that excites the Ba–Ar$_n$ system in the Σ-like state [161]. It appears that the decay channel where excited barium stays solvated into the cluster corresponds to relaxation of the excited p orbital of barium from the initial Σ-like alignment to the Π-like alignment. The same experiment shows that the initial Σ-like alignment is preserved by the desorption process, but its degree of polarization is drastically reduced. This is an indication that the desorption process is not direct. Finally, it is also found that, near the energy threshold for photodesorption, some of the surface energy of the cluster is transferred to barium, thus stimulating its ejection off the cluster.

The dynamics following photoexcitation of Ba–Ar$_n$ clusters have been investigated further for Ba–Ar$_{125}$ clusters in a molecular dynamics simulation [162]. A surface-hopping method has been used to account for the transitions between the different excited electronic states of the system. A quantum dynamics calculation has also been done on the same system for smaller clusters (Ba–Ar$_{10}$ and Ba–Ar$_{20}$) [163]. The dynamics of the coupled electronic–nuclear motions in the cluster involves transitions between the three potential energy surfaces corresponding to the different alignments of the excited p orbital of barium. The calculations confirm the suggestions made from the experimental results. Upon electronic excitation, energy is rapidly redistributed in the cluster and no direct ejection of barium occurs for large clusters. The electronic relaxation to the lowest P state (i.e. to the Π-like state according to the pseudo-diatomic picture) is mostly complete in less than 10 ps but does not start immediately upon laser excitation. The calculation performed on small clusters indicates that the electronic relaxation becomes appreciable about 1 ps after the photoexcitation. In large clusters, ejection of barium is a rare and delayed event that occurs when a dynamical fluctuation creates a *hot spot* at the barium site, simultaneously with a non-adiabatic excitation to the upper P state. Only the smallest clusters (Ba–Ar$_{10}$) are associated with a large photodesorption probability of barium, and in that case the photodesorption is direct. No experiment has been performed yet on sufficiently small clusters to confirm these predictions.

4.2. *Photodissociation of the guest molecule*

The simplest chemical reaction is photodissociation of a diatomic molecule; a single bond is broken, and no ambiguity exists on the nature of the reaction coordinate. For this reason, an impressive body of literature is devoted to the effect of an environment on photodissociations. It is impossible to review it thoroughly here, and we focus only on photodissociation of halogen molecules within rare-gas solvents.

Particular emphasis has been given to photodissociation of halogen molecules (Cl_2 or I_2) in rare-gas solvents, both in experimental [26, 164–173] and theoretical [174–181] studies. The most recent experimental studies in that field have been performed in the time domain with the aim of documenting two solvent properties: the cage and chaperon effects. Several of the time-resolved experiments performed so far have been

conducted on clusters [26, 167–169, 173], the photodissociation being probed either by detecting the halogen molecule that recombines after photodissociation [167, 169, 172] or by detecting one of the halogen fragment atoms as it travels through and exchanges kinetic energy with the rare-gas environment [26, 173, 182]. Work has been done in our group to document the photodissociation of Cl_2 molecules in the environment of xenon and argon atoms [182]. The real-time pump-probe and laser-induced fluorescence detection techniques have been used to investigate both the photodissociating Cl_2 ($^{1,3}\Pi_u$) molecule and the chlorine atoms moving close to xenon atoms. The photodissociation process is direct for free Cl_2. In contrast, it is considerably slowed down and takes 750 fs in large clusters.

4.3. *Association reactions between guest atoms or molecules*

The pick-up technique offers the possibility of attaching several guests on the same host. Owing to the low temperature of van der Waals clusters, association between guest particles is therefore anticipated. Such behaviour has been observed experimentally for the first time with the dimerization of CH_3F molecules in argon clusters [183, 184]. Similarly, CF_3Cl molecules associate at the surface of argon clusters [154].

Molecular association on cold clusters has recently been investigated in molecular dynamics calculations [139]. It has been found that collisions between N_2O molecules at the surface of large argon clusters result in fast sequential clustering of the host molecule [139].

Several groups are active along this line. For example, Huisken and Stemmler [134] have investigated electron impact mass spectra and, more interestingly, infrared spectra of small methanol clusters (dimers, trimers and tetramers) embedded in large argon clusters. They found that methanol dimers and trimers adopt the same structure on the argon cluster as in the gas phase, whereas the tetramer behaves differently.

Furthermore, an association reaction has also been observed between chemically different guest molecules deposited on the same cluster, namely hydrogen-bond formation between a CH_3F molecule and a HCl molecule. The reaction has been monitored by infrared spectroscopy. The association reaction proceeds to completion in the time window of the experiment (100 μs) [184].

Association reactions between metal atoms have also been reported. We have seen in section 3.1.2 that laser-induced fluorescence of barium atoms adsorbed on argon cluster reveals indirectly the association between two or more metal atoms on a cold argon cluster. Sodium dimers and trimers have also been detected very recently in helium clusters and their electronic spectroscopy has been investigated thoroughly [185]. Here again, as mentioned above for the electronic excitation of guest atoms in argon clusters, the electronic excitation of the alkali dimers and trimers in helium clusters is close to that of the isolated molecule. Only a cluster-induced broadening of the vibrational bands is observed [185, 186].

Lewerenz *et al.* [187] have reported the clustering of up to 30 guest atoms or molecules. The experiment has been conducted by crossing a beam of large helium clusters ($He_{>1000}$) with a buffer gas: argon, krypton, xenon H_2O or SF_6. In spite of the very low temperature of helium clusters (0·4 K) the clustering of the guest particles is not complete. This very surprising result has been interpreted as due to solvation of several guest particles at different sites in the interior of the helium cluster, forming what Leverenz *et al.* called 'cluster seeds'. The incomplete clustering of the guest molecules indicates that different *seeds* on the same cluster do not recombine in the

time scale of the experiment. An explanation is that 'cluster seeds' could be formed of a dense shell of helium atoms around a single guest molecule that impedes the recombination of several guest molecules.

Cluster hindrance to molecular recombination has been encountered as a possible signature of melting-like transitions in clusters. Classical trajectory calculations on the HCl formation in collisions of hydrogen atoms with $Cl(Ar)_{12}$ clusters have shown that, in the solid-like phase of the cluster at low temperatures ($T < 40$ K), there is strong screening of the chlorine atom by the icosahedral argon solvation shell, preventing the H+Cl association reaction from being observed. In contrast, a large reactivity is found when the cluster is liquid like ($T \approx 45$ K) [188, 189].

5. Cluster isolated chemical reaction, a quantitative way of studying reaction dynamics in clusters

The CICR method was developed in our laboratory. It allows one to observe the behaviour of a specified number of reactants in the environment of a large atomic or molecular cluster. The principle of the method and the apparatus used to performed CICR studies are detailed in section 5.1. Four points serve to structure the review of the results obtained so far in our laboratory.

(1) We first establish that two reactants deposited on the same cluster do explore the cluster surface, eventually collide each other and react (section 5.2).
(2) We investigate the time interval between reactant–reactant collisions on clusters (section 5.3).
(3) Then we come to the main problem of the CICR method: do clusters affect reaction dynamics? This question is answered by considering both very exoergic reactive and non-reactive collisions (section 5.4).
(4) Finally results are shown where argon clusters are used to stabilize small barium clusters in order to explore their reactivity (section 5.5).

5.1. *Overview of the method*

5.1.1. *Apparatus*

The experimental set-up is shown in figure 1. It has been described in [190]. Briefly, clusters are generated by supersonic expansion of argon, methane or nitrogen into vacuum. The right choice of the source backing pressure (3–40 bar) and nozzle temperature (200–300 K) allows the average size of the clusters to be varied between a few hundred and several thousands of particles. The cluster size is determined using the techniques described in section 2.1.2.

Addition of reactants to the clusters is performed by the pick-up technique. This can be done at different locations along the beam path, either in the region between the skimmer and the collimator that define the beam, or after the collimator inside the main chamber where the measurements are performed. The cluster beam crosses two pick-up zones in the main chamber. The first is a barium cell that allows barium atoms to be deposited on the clusters. The second pick-up zone is provided by an effusive beam that crosses the cluster beam. The average number of each reactant deposited per cluster is determined using one of the methods described in section 3.1.2.

The crossing zone between the cluster beam and the effusive beam is also crossed by the output of two optical fibres in order to illuminate this region, when needed, with one or two tunable lasers. Finally, this zone is imaged on the entrance slit of a monochromator for the purpose of fluorescence measurements. One of the tools used

① is the source chamber ② is a chamber of differential pumping
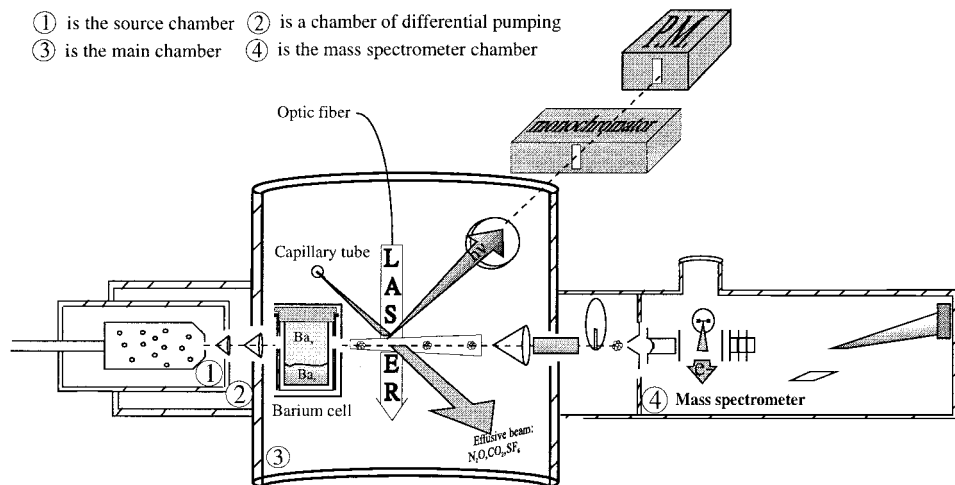③ is the main chamber ④ is the mass spectrometer chamber

Figure 1.   Scheme of the experimental set-up.

to monitor the reaction dynamics that takes place in the cluster is indeed based on fluorescence measurements.

The cluster beam then enters a chamber that contains a chopping wheel and then into another chamber equipped with mass spectrometers (a time-of-flight mass spectrometer and a quadrupole mass spectrometer). A compression chamber can be interposed in the beam path in front of the mass spectrometer in order to destroy the cluster and to measure the partial flux of the species forming the cluster. Our second tool to monitor reaction dynamics in clusters is mass spectrometry.

5.1.2. *Types of experiment allowed by the apparatus*

The first category of experiments corresponds to spectroscopy and photo-desorption. In this case, the reactants of only one species are added to the cluster. The corresponding results have already been reported in sections 3.2.1 and 4.1.

The present section is centred on studies performed when two different reactant species are deposited on the cluster. This allows one to investigate CICRs.

Qualitatively, the CICR principle is to deposit two kinds of reactant, say a barium atom and a N_2O molecule on the same cluster (an argon cluster for instance), thus forcing them to explore a finite space and to react at the contact of the cluster. Observation of the reaction product yields information on the dynamics of the cluster reaction.

We have seen in section 3.1.2 that the number of reactants picked up by the clusters is distributed according to the Poisson law. As a result, whatever the average number $\langle m \rangle$ of reactants per cluster, the beam contains a distribution (varying with $\langle m \rangle$) of clusters carrying zero, one, two, three, etc., reactants. The observed reaction signals can therefore be originating from clusters carrying one, two three, etc., reactants of each type. For this reason, we made the CICR method quantitative.

Quantitative CICR consists in recording reaction signals as a function of the average number of one of the reactants deposited per cluster and to fit them by the appropriate Poisson distribution function $P_1 (\langle m \rangle)$, $P_2 (\langle m \rangle)$, $P_3 (\langle m \rangle)$, etc., thus determining unambiguously whether the signal originates from clusters carrying one, two, three or more reactant particles. In other words, quantitative CICR informs directly on the stoichiometry of the reaction.

A rapid consideration may suggest that quantitative CICR works very much like standard studies in macroscopic reaction media where reactive signals are monitored as a function of a macroscopic state variable, partial pressure or concentration. An important difference must be emphasized. In macroscopic media, a linear variation in the reaction signal with one of the reactants does not necessarily imply that only one molecule of this reactant is involved in the reaction. The reaction may indeed be pseudo first order with respect to this reactant when the reaction has multiple steps. In contrast, quantitative CICR experiments lead to unbiased information on the reaction stoichiometry because they deal with the true number of reactants through Poisson laws rather than simply with the variation in a macroscopic number of reactants. Of course, this situation is encountered because the reaction medium in CICR experiments is of both finite and microscopic size.

Two variants of the CICR are used in our apparatus. They differ in the choice of signal that is used to monitor the reaction.

First we can measure the decrease in abundance of one kind of reactant when adding more and more of the second reactant to the cluster. Such a measurement is achieved by recording reactant fluxes using the compression chamber set in front of the mass spectrometer. This documents the stoichiometry of the total reaction, whatever the nature and the internal state of the reaction products.

Second, by recording a chemiluminescence signal as a function of the average number of both reactants on the cluster, the stoichiometry of the chemiluminescent channel that is observed can be documented.

5.2. *Large clusters acting as reaction media*

The Ba–N_2O system has been chosen as a prototypical reaction to examine how clusters of various chemical natures can act as reaction media.

5.2.1. *Reaction products*

The reaction

$$Ba(6s^2\,{}^1S_0) + N_2O \rightarrow BaO + N_2, \quad \Delta H_0 = -4{\cdot}1\ eV, \qquad (12)$$

has been extensively investigated in the gas phase. Its large branching ratio for chemiluminescence indeed anticipates its use for chemical lasers. The chemiluminescent product is BaO in the electronic states A ${}^1\Sigma$, A$'$ ${}^1\Pi$ and a ${}^3\Sigma$. The resulting chemiluminescence is shown in the insert of figure 2. It is a broad fluorescence that covers most of the visible region. It reflects the large exoergicity of the reaction that leads to electronic excitation of the product BaO with a large vibrational and rotational energy.

We have attached both N_2O molecules and barium atoms to large argon clusters [140, 191]. The observed chemiluminescence is shown in figure 2 for two different average sizes of the cluster: $Ar_{\bar{n}=300}$ and $Ar_{\bar{n}=2000}$. The spectrum presents two components that are both assigned to BaO emission. One extends between 550 and 850 nm. It is very structured and is superimposed on a broad unstructured spectrum that is a reminiscence of the hot gas-phase product. These components do not scale together when the cluster size is varied, implying that they have independent origins. We have shown that the unstructured component is due to emission of hot BaO molecules that have been formed by the Ba + N_2O reaction on the cluster and that have left the cluster immediately upon reaction. The structured component is associated with BaO molecules that stay solvated in the argon cluster. These molecules are
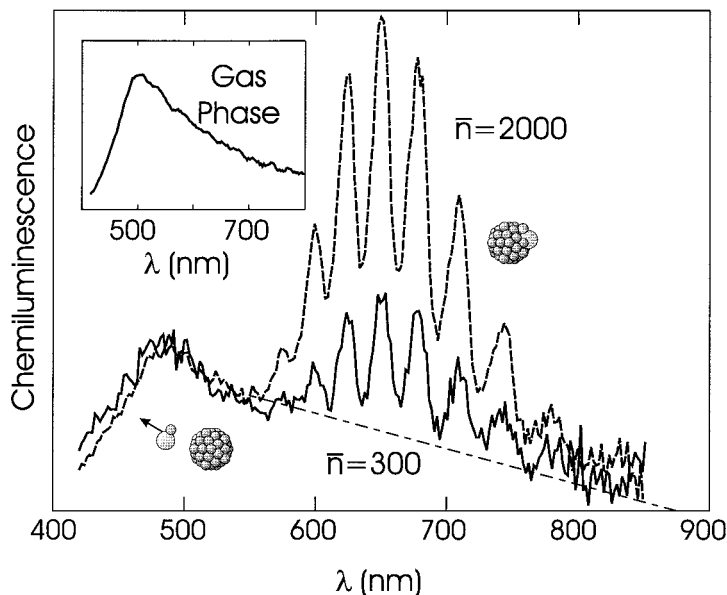
Figure 2. Chemiluminescence spectra recorded in the $(Ba + N_2O) Ar_{\bar{n}=2000}$ and $(Ba + N_2O)$ $Ar_{\bar{n}=300}$ reactions as labelled in the figure. The spectra are corrected for background signals, for the transmission of the optics and monochromator, and for the response of the photomultiplier. The inset shows the chemiluminescence of the gas-phase $Ba + N_2O$ reaction.

certainly very hot just after the reaction but, before they emit fluorescence, they are cooled rotationally and vibrationally by partly evaporating the cluster. Such evaporative cooling has been modelled on a different system by Hu and Martens [192] in a classical trajectory calculation of the $I - Ar_n + I \rightarrow I_2 + nAr$ reaction. The two locations of the BaO emitter are shown schematically in figure 2.

5.2.2. *Effect of varying the nature of the cluster*

The $Ba + N_2O$ reaction has been studied under different cluster environments.

(1) *Argon clusters* [140, 191] as reported above where chemiluminescence corresponding to solvated BaO molecules appears as a structured vibrational progression (see figure 2). Interaction of the product BaO with the surrounding argon atoms reduces the ground-state vibrational constant ω_e from 669·76 cm^{-1} to 654 ± 3.5 cm^{-1} [191].

(2) *Methane clusters* [193]. Both components are observed and the fluorescence yield is comparable with that observed in argon cluster experiments. However, the emission of solvated BaO is unstructured, revealing association of the BaO product with at least one CH_4 molecule.

(3) *Nitrogen clusters* [190]. Only emission of free BaO is observed and the chemiluminescent yield at 500 nm is six times smaller than in argon clusters.

(4) *N_2O clusters* [67]. No chemiluminescence is observed.

These results can be rationalized by assuming that the chemiluminescence yield of solvated BaO is directly affected by the strength of its interaction with the surrounding cluster [190]. Argon has a fairly weak interaction that shifts only the vibrational progression. The stronger interaction with methane washes out the structure of the progression. In contrast, nitrogen that may capture a valence electron of BaO through
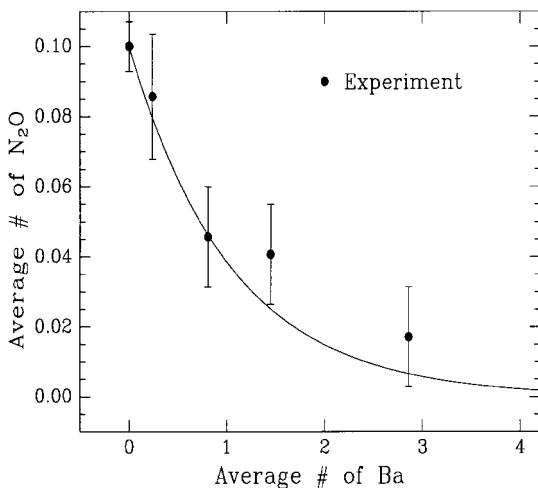
Figure 3. Average number of N_2O molecules left on $Ar_{\bar{n}=6000}$ clusters when the average number $\langle m \rangle_{Ba}$ of barium atoms is varied. The points with error bars are the experimental results. The full curve is the zero-order Poisson distribution $P_0(\langle m \rangle_{Ba})$.

the 2 eV resonance in $e^- - N_2$ scattering, totally quenches the chemiluminescence of solvated BaO. Finally the interaction of BaO with a N_2O cluster is probably even stronger because N_2O has a permanent dipole. All chemiluminescent channels are quenched in that case.

5.2.3. *Efficiency of the cluster as a microreactor*

The above results illustrate that, when two reactants are deposited on the same cluster, their relative mobility is large enough for a reaction to occur. The next step is to determine the reaction probability itself. This has been possible by measuring the amount of N_2O molecules consumed by the reaction when varying the average number of barium atoms deposited per cluster. The experiment is conducted as follows. The reactants N_2O and barium are deposited on the argon clusters. Then, the clusters are scattered in the compression chamber and the partial pressure of N_2O is measured by mass spectrometry as a function of the average number of barium atom per cluster. The partial pressure of N_2O thus reflects directly the average number of unreacted N_2O that are left on clusters. The corresponding results are shown in figure 3 for an experiment where an average of 0·1 N_2O molecules per cluster was deposited prior to barium deposition. The low value of the initial N_2O coverage prevent complications with clusters carrying more than one N_2O molecule. As expected, the average number of N_2O molecules left per cluster decreases as $\langle m \rangle_{Ba}$ is increased. The important point is that the decay is adequately fitted by the Poisson distribution P_0 $(\langle m \rangle_{Ba})$. This indicates that only clusters containing no barium atoms are able to transport N_2O molecules from the pick-up region to the compression chamber. Conversely, clusters that contain both N_2O and barium do not carry N_2O into the compression chamber. This suggests that the N_2O molecules have reacted within 100% completion with the barium atoms before the clusters have entered the compression chamber. The fact that the reaction occurs with unit probability on the cluster is a strong indication that the reaction has no barrier higher than the cluster temperature along the reaction coordinate.

The picture that we have arrived at at this point is the following. When the two

reactants (say, barium and N_2O) are deposited on the same cluster, they have enough relative mobility to collide, possibly more than once, and to react in the time window of the experiment (a few milliseconds) when the reaction has no barrier. Other chemiluminescent reactions of barium atoms have been explored on argon [194] and methane clusters [193]. The results obtained agree with the present picture. Such a picture has also been confirmed recently by molecular dynamics calculations. Gaigeot *et al.* [139] have found indeed that one N_2O molecule and one barium atom need an average time of 25 ns to collide each other on the surface of an Ar_{1000} cluster. So the time scale for collisions is actually very small compared with the time window of the experiment as anticipated from the experimental work.

5.3. *Time scale for collisions in clusters*

The previous section gave an upper limit of the relative mobility between reactants in argon clusters. To proceed further and to obtain a more accurate estimate of this mobility, we compare it with radiative emission that has a known time scale. We have investigated the collision quenching of $Ba(6s6p\ ^1P_1)$ by CH_4 and a few other molecules so as to quantify the relative mobility of $Ba(6s6p\ ^1P_1)$ and CH_4 within argon clusters [142, 195]. The time scale in this experiment is set by the radiative lifetime of $Ba(6s6p\ ^1P_1)$ ($\tau = 8$ ns [196]). The experiment consists in exciting barium in the cluster at 544 nm and to record the barium fluorescence as a function of the average number $\langle m \rangle_{CH_4}$ of methane molecules deposited per cluster. Methane is believed to be a good quencher of the barium electronic excitation. Therefore a single collision between barium and methane is enough to quench the electronic excitation. The decay of the fluorescence as a function of $\langle m \rangle_{CH_4}$ thus documents the collision rate between barium and methane on clusters. The relation between fluorescence decay and collision rate k has been derived in [142]. Quantitatively, the value of $k = 7 \cdot 5 \times 10^7$ s^{-1} is found in an experiment on $Ar_{\bar{n}=420}$ clusters. This value is very large. It corresponds to the exploration of the cluster in 13 ns. This indicates surface mobility of the collision partners, in agreement with the following observation: the exploration time scales as the cluster surface when varying the size of the cluster [195].

5.4. *Influence of the cluster on collision dynamics*

The central point in studying reaction dynamics in clusters is to determine whether and how the reaction dynamics are affected by the cluster. Several collision processes have been studied in our laboratory to shed light on this question.

5.4.1. *Argon clusters, spectators in the exit channel of quenching collisions of* $Ba(6s6p\ ^1P_1)$

The collisional deactivation of $Ba(6s6p\ ^1P_1)$ and subsequent desorption off an argon cluster provides a first insight into the influence of an environment on collision dynamics. Such a process may not be the dominant process in excited barium–methane collisions, but it offers the unusual opportunity of investigating a collision process where interaction with the reaction medium is present both before and during the collision, but not after the collision.

The quenching process that is investigated is

$$Ba(6s6p\ ^1P_1) + CH_4 \rightarrow Ba(6s6p\ ^3P_2) + CH_4, \quad \Delta H_0 = -0 \cdot 56 \text{ eV}. \tag{13}$$
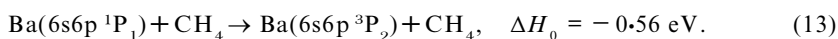
The quenching collision occurs with barium and CH_4 moving on $Ar_{\bar{n}=600}$ clusters. The role of the cluster in the quenching process is checked by measuring the recoil
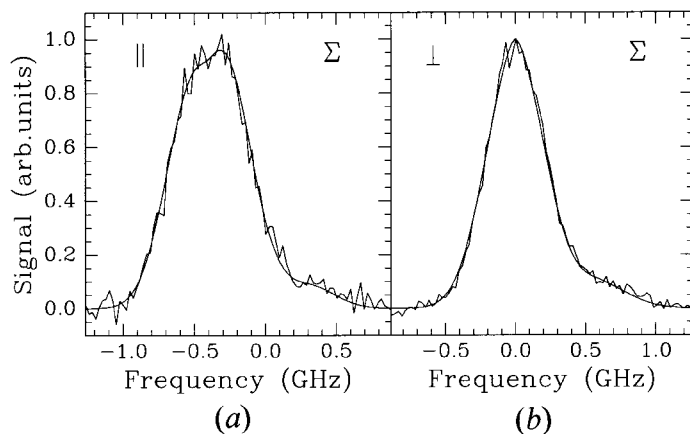
Figure 4. Doppler spectroscopy of the Ba($6s6p\,^3P_2 \to 6s7s\,^3S_1$) transition in a quenching experiment on Ar$_{\bar{n}=600}$ clusters. Barium atoms were excited through the Σ band of the Ba($6s^2\,^1S_0 \to 6s6p\,^1P_1$) absorption. Collision of Ba($6s6p\,^1P_1$) with CH$_4$ on the cluster transferred the excitation to the lower $6s6p\,^3P_2$ level of barium. Doppler spectroscopy detects free barium atoms as they desorb off the cluster after (or during) the quenching process. (*a*) and (*b*) are two different alignments of the probe laser as explained in [197]. Computer simulations of the experimental profiles are superimposed on the experimental signal. (Taken from [197].)

velocity of the Ba,($6s6p\,^3P_2$) atoms that are desorbed off the cluster [197]. Doppler spectroscopy is used for this measurement, with the probe laser tuned to the transition $6s6p\,^3P_2 \to 6s7s\,^3S_1$ of free barium.

Typical Doppler profiles are shown in figure 4. Full information on the angular and velocity distributions of desorbed barium is obtained when fitting the Doppler profiles of figure 4 (plus others obtained with a different alignment of the pump laser) by a model that takes into account the experimental averagings and the temporal saturation effects [198]. The model was built following [199]. The picture that emerges from the fits is the following. The Ba–CH$_4$ quenching collisions at the cluster surface behave very much like gas-phase collisions at the temperature of the cluster (32 K). In other words, the cluster was present in the entrance channel of the quenching process for creating the conditions of a collision between barium and methane but took no part in the collision itself.

The situation that is created by the present experiment is very unusual, because in normal solution chemistry the solvent is present both in the entrance channel and in the exit channel of the collision. Here we are facing an example where possible coupling to the solvent exists in the entrance channel and during the collision but not in the exit channel. The results obtained for the quenching process indicate that the solvent acts as a low-temperature thermostat in the entrance channel of the collision, but not during the collision when the system moves on rapidly varying potential surfaces.

5.4.2. *Argon clusters, traps of the reaction intermediate in Ba + Cl$_2$ collisions*

This section illustrates the opposite situation to that encountered in the previous section. The cluster has enough interaction with products in the exit channel of the Ba + Cl$_2$ reaction to affect dramatically the reaction dynamics [194].

The reaction Ba + Cl$_2$ has been extensively studied in the gas phase under both the single-collision and the multiple-collision regime [200, 201]. The reaction goes through
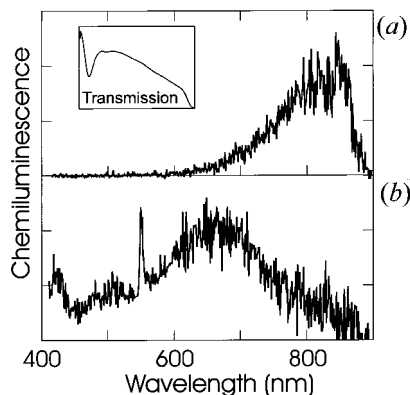
Figure 5. Chemiluminescence spectrum of the $Ba + Cl_2$ reaction. Comparison between (*a*) the gas-phase reaction and (*b*) the cluster reaction. The spectra are not corrected for the transmission efficiency of detection system shown as the inset in (*a*).
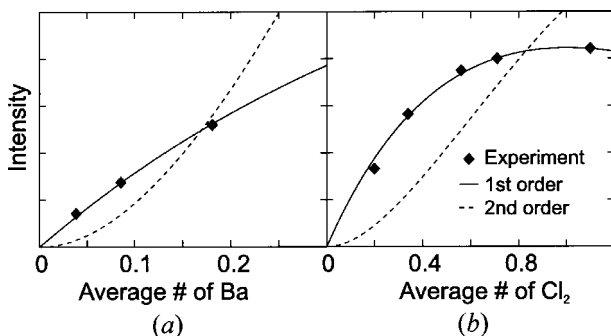
Figure 6. Chemiluminescence intensity as a function of (*a*) the average number $\langle m \rangle_{Ba}$ of barium atoms and (*b*) the average number $\langle m \rangle_{Cl_2}$ of Cl_2 molecules deposited per cluster. The curves show the variation in Poisson distributions of orders one and two as labelled in the figure.

a harpoon mechanism forming temporarily the charge-transfer complex $Ba^+Cl_2^-$. Under the single-collision regime, the complex falls apart as $BaCl + Cl$ and the reaction product $BaCl$ is formed either in the ground state or in electronically excited states and lead to chemiluminescence as shown in figure 5 (*a*).

Both barium atoms and Cl_2 molecules have been deposited on $Ar_{\bar{n}=8000}$ clusters. The observed chemiluminescence is shown in figure 5 (*b*). The emitter is obviously not the gas phase product $BaCl$. The broad unstructured spectrum that is observed makes its identification difficult. Quantitative CICR is used to help the identification. The chemiluminescence signal is studied as a function of the average number of both barium atoms and Cl_2 molecules deposited per cluster. As observed in figure 6, the chemiluminescent signal varies as the number of clusters carrying one Cl_2 molecule (Poisson distribution $P_1(\langle m \rangle_{Cl_2})$) and one barium atom (distribution $P_1(\langle m \rangle_{Ba})$) [194]. As a result, the chemiluminescence observed in figure 5 (*b*) is due to reaction of one barium atom with one chlorine molecule. Except for $BaCl$ that is not the chemiluminescence emitter, the only product that can be formed in collision of a single barium atom with a single Cl_2 molecule and that can energetically lead to the fluorescence observed is $BaCl_2$. We therefore identify $BaCl_2$ as the product in the CICR.

In this case the cluster has had a profound influence on the reaction. Indeed, the gas-phase chemiluminescent reaction under the single-collision regime is

$$Ba + Cl_2 \rightarrow BaCl(A, B) + Cl \tag{14}$$

whereas the chemiluminescent reaction of a single pair of reactants on argon clusters is
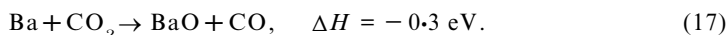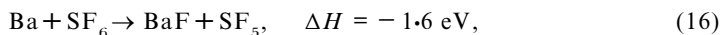
$$Ba + Cl_2 \rightarrow BaCl_2^*. \tag{15}$$

Possible reasons for this behaviour have been discussed in [194]. A likely reason involves the direct influence of the argon cluster on the reaction dynamics. Following the concept of time scale separation [202, 203], one can anticipate that the solvent is active and has a profound influence on the reaction dynamics when the movement of the reactive system along the reaction coordinate is not extremely rapid compared with the movements of the solvent molecules. In other words, the solvent is not expected to affect dramatically the reaction dynamics in the region of the transition state where movement along the reaction coordinate is expected to be rapid. In contrast, the solvent influence could be very large when the system is far from the transition state region. In the present case, the first role of the argon cluster is to prepare the collision, as in the previous section where the argon cluster acts as a thermal bath at 32 K, thus allowing for collisions between reactants at 32 K. The transition state region of the $Ba + Cl_2$ reaction corresponds to the electron transfer forming the complex $Ba^+Cl_2^-$. The argon cluster probably plays no important role during the electron transfer step. When formed in the gas phase, the $Ba^+Cl_2^-$ complex decays by dissociation of the Cl_2^- ion as $Cl^- + Cl$, thus forming the reaction the reaction product by association of the remaining Ba^+ ion with the newly formed negative ion Cl^-. Dissociation of the Cl_2^- ion is not free in argon clusters and may even be inhibited, thus stimulating the formation of the observed $BaCl_2$ product. Such a phenomenon has already been observed and studied by Lineberger's group [30–33]. Namely, recombination of the Br_2^- ion has been observed in CO_2 clusters after this ion was photodissociated in the cluster.

5.4.3. *Argon clusters*, *quenchers of gas phase chemical reactions*

The $Ba–Cl_2$ system is a primary example where the argon cluster affects dramatically the gas-phase reaction, by stopping it somewhere in the exit channel and stabilizing the reaction intermediate $BaCl_2$. The $Ba + Cl_2$ system is a primary example where the cluster has quenched the gas-phase reaction.

Ground state $BaCl_2$ is stable by 7 eV with respect to $Ba + Cl_2$. It is therefore not very surprising that interaction with the cluster is able to stop the full reaction by stabilizing such a compound. We have further investigated the quenching of gas-phase reactions by considering systems that do not have stable products as a reaction intermediate. This is the case for the $Ba–SF_6$ and $Ba–CO_2$ systems. Both systems have a gas phase reaction that goes through a long-lived complex, but neither $BaSF_6$ nor $BaCO_2$ is a very stable molecule. The gas-phase reactions are

$$Ba + SF_6 \rightarrow BaF + SF_5, \quad \Delta H = -1 \cdot 6 \text{ eV}, \tag{16}$$

$$Ba + CO_2 \rightarrow BaO + CO, \quad \Delta H = -0 \cdot 3 \text{ eV}. \tag{17}$$

We have studied the $Ba–SF_6$ and $Ba–CO_2$ systems on $Ar_{\bar{n}=6000}$ clusters. An average number of 0·8 molecule has been deposited on the cluster in the first pick-up region. A mass spectrometry experiment has been performed in order to monitor the decay of this average number as a function of the average number of barium atoms deposited
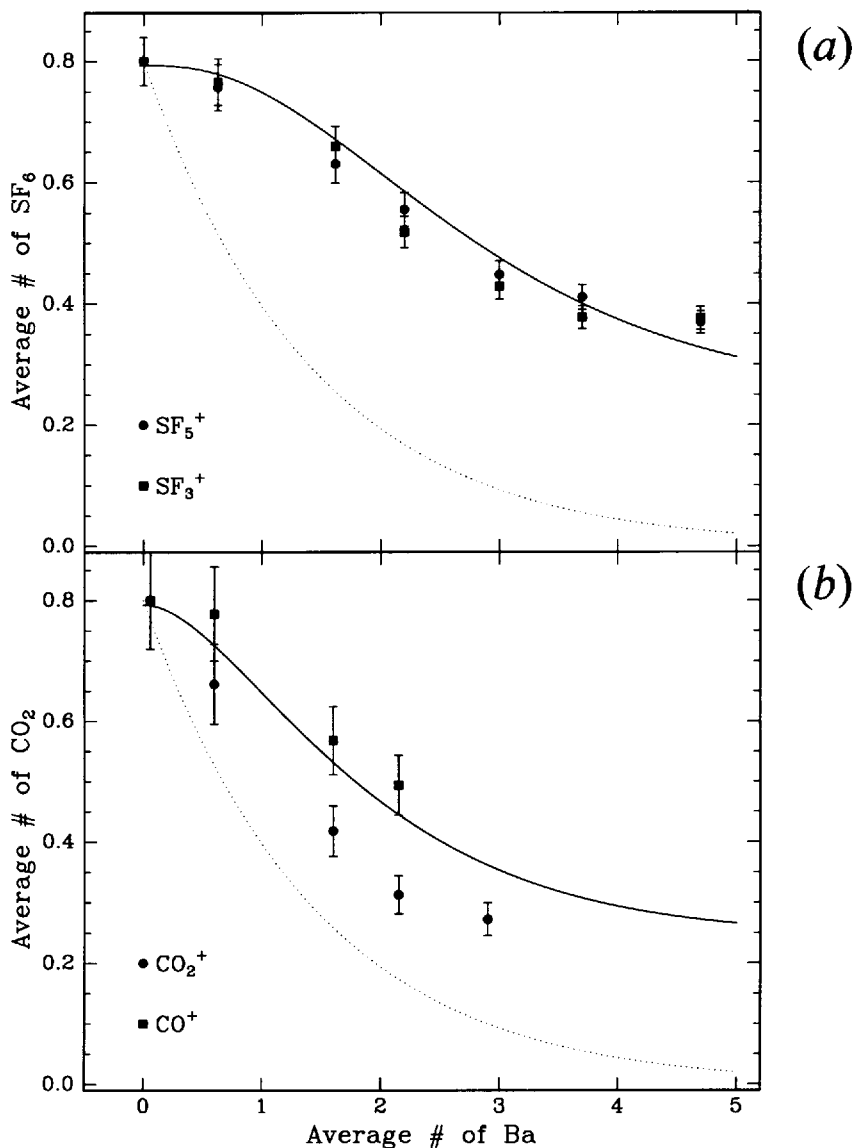
Figure 7.   Average number of (*a*) SF_6 and (*b*) CO_2 molecules left on $Ar_{\bar{n}=6000}$ clusters when the average number $\langle m \rangle_{Ba}$ of barium atoms is deposited. The points with error bars are the experimental results. The dotted curve is the zero-order Poisson distribution $P_0(\langle m \rangle_{Ba})$, and the full curve is the Poisson distribution that best fit the experimental result: $P_0(\langle m \rangle_{Ba}) + P_1(\langle m \rangle_{Ba})$ for CO_2 and $P_0(\langle m \rangle_{Ba}) + P_1(\langle m \rangle_{Ba}) + P_2(\langle m \rangle_{Ba})$ for SF_6.

on clusters in the second pick-up zone. Results are shown in figure 7. The Poisson distribution P_0 does not fit the experimental results. The results of this figure are thus qualitatively different from those encountered above in figure 3 when studying the decay of the number of N_2O molecules. In that case indeed the experimental results were nicely fitted by the Poisson distribution P_0, thus indicating 100% reaction of the barium atoms with N_2O in the time window of the experiment. In contrast, the CO_2 data are fitted by the sum of Poisson distributions $P_0(\langle m \rangle_{Ba}) + P_1(\langle m \rangle_{Ba})$, and the SF_6 data by the sum $P_0(\langle m \rangle_{Ba}) + P_1(\langle m \rangle_{Ba}) + P_2(\langle m \rangle_{Ba})$. This indicates that CO_2 molecules

are brought into the detection region by clusters carrying both zero and one barium atom. Similarly, clusters carrying as many as two barium atoms are able to bring SF_6 molecules into the detection region.

We thus conclude from the above paragraph that single barium atoms do not react with CO_2 and SF_6 in the cluster environment. Conversely, we also conclude that clusters carrying two or more barium atoms, since they did not bring CO_2 into the detection region, actually promote the Ba–CO_2 reaction. At the cluster temperature, two and more barium atoms present in the same cluster are bonded as small barium clusters. The present experiment thus indicates that barium monomers do not react with CO_2 on the argon clusters, whereas barium dimers and larger cluster do so. Similarly, the results obtained with SF_6 indicate that barium monomers and dimers do not react with SF_6 whereas trimers and larger clusters do so.

The reaction of barium clusters is the subject of the next section. The important result within this section is that the gas-phase reactions $Ba + CO_2$ and $Ba + SF_6$ are inhibited by the cluster environment.
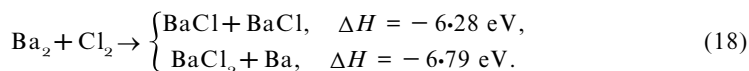
5.5. *Reactivity of small metal aggregates embedded in large argon clusters*

As a final illustration of the power of the CICR method, we review the work where argon (and nitrogen) clusters have been used to stabilize small barium aggregates (Ba_2, Ba_3, etc.), in order to explore their reactivity with oxidizing species [144, 190, 204]. Considering the temperature of argon clusters (32 K), two or more barium atoms present on the same cluster are likely to be associated as a small barium cluster. For instance the binding energy of Ba_2 has recently been calculated to be 0·2 eV [143], a value that is much larger than the thermal energy available on clusters.

The quantitative use of the CICR method finds its full power in these studies. Again, the idea is to attach barium atoms and molecular reactants to the cluster and to monitor reaction signals as a function of the average number of reactants deposited per cluster. A signal that varies as the Poisson distributions $P_2(\langle m \rangle_{Ba})$, $P_3(\langle m \rangle_{Ba})$, etc., is thus attributed to reactions of Ba_2, Ba_3, etc. The CICR method thus offers a way of exploring the reactivity of small selected metal aggregates.

This technique has been used to study the reactivity of barium aggregates with molecules ranging from very good to very poor oxidizing agents: Cl_2, O_2, CO_2 and SF_6 [144, 190, 204].
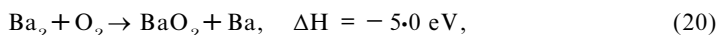
Molecular chlorine is a very good oxidizing agent. It leads to multiple chemi-luminescent channels when reacting with barium dimers. They correspond to the electronically excited products BaCl, $BaCl_2$ and Ba that are energetically accessible from the reactions [144]

$$Ba_2 + Cl_2 \rightarrow \begin{cases} BaCl + BaCl, & \Delta H = -6 \cdot 28 \text{ eV}, \\ BaCl_2 + Ba, & \Delta H = -6 \cdot 79 \text{ eV}. \end{cases} \tag{18}$$

In contrast, the chemiluminescence signals in the reaction of Ba_2 with O_2 yields BaO emission from

$$Ba_2 + O_2 \rightarrow BaO + BaO, \quad \Delta H = -6 \cdot 5 \text{ eV}, \tag{19}$$
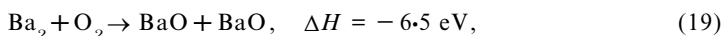
whereas the less exoergic channel

$$Ba_2 + O_2 \rightarrow BaO_2 + Ba, \quad \Delta H = -5 \cdot 0 \text{ eV}, \tag{20}$$

does not lead to observable chemiluminescence from BaO_2, although energetically allowed to do so [144].
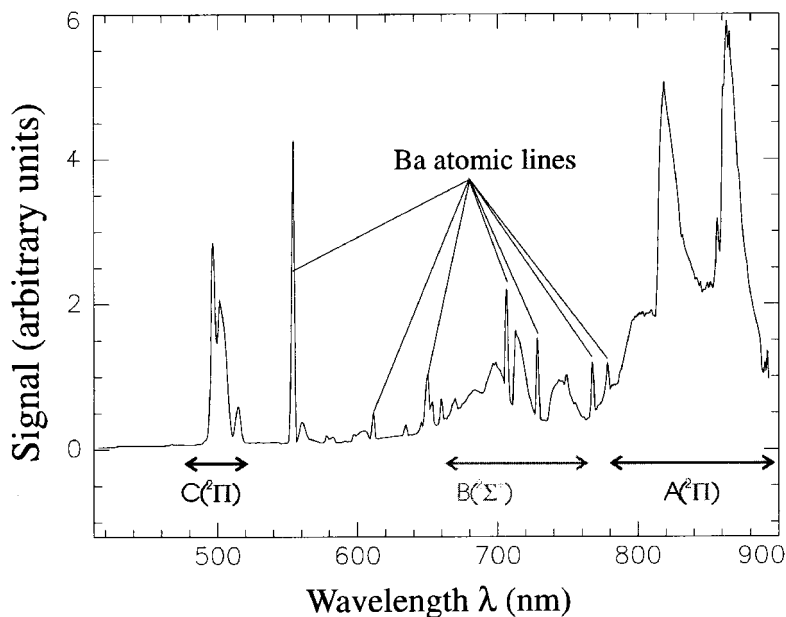
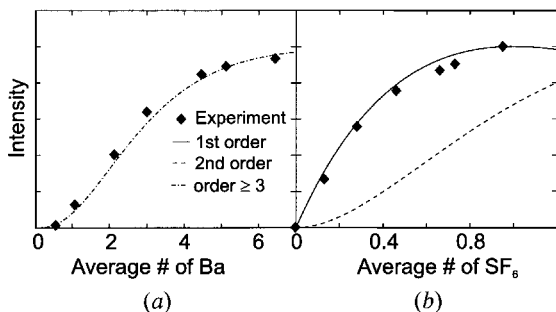Figure 8.   Chemiluminescence observed with Ba–SF$_6$ mixtures on argon clusters.

Figure 9.   Chemiluminescence intensity as a function of (*a*) the average number $\langle m \rangle_{Ba}$ of barium atoms and (*b*) the average number $\langle m \rangle_{SF_6}$ of SF$_6$ molecules deposited per cluster. The curves show the variation in Poisson distributions of various orders as labelled in the figure.

CO$_2$ and SF$_6$ molecules are poor oxidizing agents. We have observed in section 5.4.3 that barium atoms do not react with these molecules at the cluster temperatures. In contrast, Ba$_{\geqslant 2}$ aggregates react with CO$_2$, and Ba$_{\geqslant 3}$ aggregates react with SF$_6$ [190, 204]. The situation is exemplified further by considering the chemiluminescent reactions of the Ba–SF$_6$ system. Reactions of both Ba and Ba$_2$ with SF$_6$ are allowed energetically to form the chemiluminescent product BaF, and no chemiluminescence is observed experimentally. Only Ba$_3$ and larger clusters lead to chemiluminescence. The chemiluminescence spectrum is shown in figure 8. The variation in the chemiluminescence intensity is shown in figure 9 as a function of the average number of both reactants on the cluster. It proves that the observed chemiluminescence originates from reactions of one SF$_6$ molecule with Ba$_{\geqslant 3}$ aggregates.

   We are thus left with the conclusion that small barium aggregates are better reducing agents than atomic barium is. This may be understood by considering that

barium aggregates can more easily transfer an electron in a redox reaction than barium atoms. Chevaleyre [205] has indeed measured the ionization potential of small barium aggregates and found 4·2, 4·0, 4·0 and 3·6 eV for Ba_2, Ba_3, Ba_4 and Ba_5 respectively, whereas the ionization potential of barium is 5·2 eV.

6. Concluding remarks

CICR experiments appear as an interesting new direction for investigating the effect of a surrounding on reaction dynamics. Some of the work done so far using this technique demonstrates that large van der Waals clusters can actually be used as a reaction medium for studying chemical reactions at low temperatures. CICR experiments benefit of the finite size of clusters at two levels. Firstly, the finite cluster size enables one to isolate one pair of reactants in the solvent surroundings with no possible perturbation by other molecules, except of course when perturbing molecules are intentionally added to the cluster in order to explore their effects on reactivity. Secondly, a very important advantage is the possibility of depositing a controlled average number of reactants per cluster and therefore to obtaining direct quantitative information on the stoichiometry of the chemical process under study. Both advantages have been exemplified in the present review by considering the reactivity of barium atoms and small barium clusters with simple molecules such as N_2O, O_2, Cl_2, CO_2 and SF_6.

Most of the CICR experiments that have been reported have considered chemiluminescent chemical reactions. Two routes are currently developed to bypass this limitation. One has already been presented in this review. It goes through mass spectrometry detection of either the appearance of reaction products or the disappearance of the reactants. The other route is laser-induced fluorescence detection of the reaction products. Work is in progress that uses Doppler spectroscopy to determine the velocity of products that evaporate off the cluster after being produced by the reaction. Such work is directly in line with the purpose of CICR experiments; Doppler spectroscopy indeed, can be used for both detecting reaction products in the gas phase reaction and in the CICR. The comparison of both yields directly the desired information on the modification brought by clusters on reaction dynamics.

Several developments and applications of CICR-type experiments may be anticipated.

An interesting new direction would be the use of infrared spectroscopy to detect and to identify reaction products in clusters, in about the same way as done in matrix isolation experiments [29]. Unfortunately, infrared spectroscopy is not very sensitive, and the low densities that prevail in cluster beams preclude its use as a routine detection tool. A possibility would be to condense the cluster beam on a cold surface after reactants have been deposited and have reacted on clusters. This should pertain for depositing macroscopic quantities of products, and infrared spectroscopy could be used more easily.

Generating molecular beams of either non-volatile materials or heat sensitive molecules is always difficult. The high temperatures needed to obtain intense beams in the first case are not easy to achieve. Moreover, high-temperature beam sources may generate appreciable quantities of metastable particles in low lying electronic levels. In the second case, the operating temperature of the source may be too high for not destroying the molecule. A CICR-type experiment may be an interesting alternative in both cases. The requisite temperature indeed is much lower for operating the pick-up

cell than for generating a beam. Investigating the reactivity of heat-sensitive molecules (biomolecules for instance), of non-volatile materials and even of clusters of non-volatile materials can then been done together the route opened in the present work.

Finally, we have seen that, by varying the pick-up pressure, it is possible to adjust the average number of reactant particles deposited per large van der Waals cluster. Owing to the low cluster temperature, several reactants present on the same cluster are grouped together as small aggregates of known average size. The example reported above for a study of Ba_2 and Ba_3 reactivity is typical of this. Rather than using this property to study reactivity, one can use it to transport and to deposit small metallic aggregates of known average size on surfaces. In such perspective, the van der Waals cluster would be vaporized totally upon collision of the beam with a room-temperature surface, and only the small metallic aggregates would stick to the surface.

As we can see, experimental procedures derived from CICR experiments with careful control of the pick-up conditions may lead to applications far beyond the field of reaction dynamics that was the scope of the present review.

References

[1] LEVINE, R. D., and BERNSTEIN, R. B., 1987, *Molecular Reaction Dynamics and Chemical Reactivity* (Oxford University Press).

[2] FAUBEL, M., MARTINEZ-HAYA, B., RUSIN, L. Y., TAPPE, U., and TOENNIES, J. P., 1995, *Z. phys. Chem.*, **188**, 197.

[3] FAUBEL, M., MARTINEZ-HAYA, B., RUSIN, L. Y., TAPPE, U., and TOENNIES, J. P., 1995, *Chem. Phys. Lett.*, **232**, 197.

[4] BUCHENAU, H., TOENNIES, J. P., ARNOLD, J., and WOLFRUM, J., 1990, *Ber. Bunsenges. phys. Chem.*, **94**, 1231.

[5] BISHOP, D. M., 1994, *Int. Rev. phys. Chem.*, **14**, 21.

[6] BEN-NUN, B., and LEVINE, R. D., 1994, *Int. Rev. phys. Chem.*, **14**, 215.

[7] JORTNER, J., LEVINE, R. D., and RICE, S. A., 1988, *Adv. chem. Phys.*, **70**, 1.

[8] JORTNER, J., SCHARF, D., BEN-HORIN, N., EVEN, U., and LANDMAN, U., 1990, *The Chemical Physics of Atomic and Molecular Clusters*, Proceedings of the International School of Physics Enrico Fermi Course CVII edited by G. Scoles (Amsterdam: North-Holland), pp. 43–98.

[9] JORTNER, J., 1992, *Z. Phys.* D, **24**, 247.

[10] HABERLAND, H., (editor), 1993, *Clusters of Atoms and Molecules I* (Berlin: Springer).

[11] HABERLAND, H., (editor), 1994, *Clusters of Atoms and Molecules II* (Berlin: Springer).

[12] JORTNER, J., 1995, *J. Chem. phys.*, **92**, 205.

[13] PASTOR, G. M., and BENNEMANN, K. H., 1993, *Clusters of Atoms and Molecules I*, edited by H. Haberland (Berlin: Springer), chapter 2. 4, pp. 86–113.

[14] 'Large Gas-phase Clusters', 1990, *J. chem. Soc. Faraday Trans.*, **13**.

[15] JORTNER, J., PULLMAN, B., and LEVINE, R. D., (editors), 1993, *Reaction Dynamics in Clusters and Condensed Phases*, Jerusalem Symposia on Quantum Chemistry and Biochemistry, No. 26 (Dordrecht: Kluwer).

[16] (a) GERBER, R. B., McCOY, A. B., and GARCIA-VELLA, A., 1994, *A. Rev. phys. Chem.*, **45**, 275. (b) MARCUS, R. A., 1996, *J. chem. Phys.*, **105**, 5446.

[17] TRAMER, A., and SOLGADI, D., (editors), 1995, *J. Chim. phys.*, **92**.

[18] KNOCHENMUSS, R., 1995, *J. Chim. phys.*, **92**, 445.

[19] KIM, S. K., BREEN, J. J., PENG, L. W., HEIKAL, A., SYAGE, J. A. and ZEWAIL, A. H., 1995, *J. phys. Chem.*, **99**, 7421.

[20] WÖRMER, J., KAMBACH, R., JOPPIEN, M., and MÖLLER, T., 1996, *J. chem. Phys.*, **104**, 8269.

[21] SHIN, S. K., CHEN, Y., NICKOLAISEN, S., SHARPE, S. W., BEAUDET, R. A., and WITTIG, C., 1991, *Adv. Photochem.*, **16**, 249.

[22] BRECKENRIDGE, W. H., JOUVET, C., and SOEP, B., 1995, *Adv. Metal Semicond. Clusters*, **3**, 1–83.

[23] JOUVET, C., and SOLGADI, D., 1996, *Reaction in Clusters*, edited by E. R. Bernstein, (Oxford University Press).

[24] DEDONDER-LARDEUX, C., JOUVET, C., MARTRENCHARD-BARRA, S., and SOLGADI, D., 1997, *Adv. Multiphoton Spectrosc.* **10** (to be published).

[25] BERNSTEIN, E. R., 1992, *J. phys. Chem.*, **96**, 10105.

[26] RETTIG, W., DEDONDER-LARDEUX, C., JOUVET, C., MARTRENCHARD-BARRA, S., SZRIFIGER, P., KRIM, L., and CASTANO, F., 1995, *J. Chim. phys.*, **92**, 465.

[27] SYAGE, J. A., 1994, *Z. phys. D*, **30**, 1.

[28] SYAGE, J. A., 1995, *J. phys. Chem.*, **99**, 5772.

[29] BONDYBEY, V. E., SMITH, A. M., and AGREITER, J., 1996, *Chem. Rev.*, **96**, 2113.

[30] RAY, D., LEVINGER, N. E., PAPANIKOLAS, J. M., and LINEBERGER, W. C., 1989, *J. chem. Phys.*, **91**, 6533.

[31] PAPANIKOLAS, J. M., GORD, J. R., LEVINGER, N. E., RAY, D., VORSA, V., and LINEBERGER, W. C., 1991, *J. phys. Chem.*, **95**, 8028.

[32] PAPANIKOLAS, J. M., VORSA, V., NADAL, M. E., CAMPAGNOLA, P. J., GORD, J. R., and LINEBERGER, W. C., 1992, *J. chem. Phys.*, **97**, 7002.

[33] PAPANIKOLAS, J. M., VORSA, V., NADAL, M. E., CAMPAGNOLA, P. J., BUCHENAU, H. K., and LINEBERGER, W. C., 1993, *J. chem. Phys.*, **99**, 8733.

[34] CASTLEMAN, A. W. JR., 1994, *Clusters of Atoms and Molecules*, edited by H. Haberland (Berlin: Springer), part 2.2.4.

[35] ZHU, X. Y., 1994, *A. Rev. phys. Chem.*, **45**, 113.

[36] POLANYI, J. C., and ZEIRI, Y., 1995, *Laser Spectroscopy and Photochemistry on Metal Surfaces*, edited by H. L. Dai and W. Ho (Singapore: World Scientific), p. 1241.

[37] BARCLAY, V. J., HUNG, W. H., KEOGH, W. J., KÜHNEMUTH, R., POLANYI, J. C., JENNISON, D. R., and LI, Y. S., (1996), *J. chem. Phys.*, **105**, 5005.

[38] HARTMANN, M., MIELKE, F., TOENNIES, J. P., VILESOV, A. F., and BENEDEK, G., 1996, *Phys. Rev. Lett.*, **76**, 4560.

[39] HUISKEN, F., and STEMMLER, M., 1992, *Z. Phys. D*, **24**, 277.

[40] BUCK, U., SCHMIDT, B., and SIEBERS, J. G., 1993, *J. chem. Phys.*, **99**, 9428.

[41] BUCK, U., and HOBEIN, M., 1993, *Z. Phys. D*, **28**, 331.

[42] BUCK, U., HOBEIN, M., and SCHMIDT, B., 1993, *J. chem. Phys.*, **98**, 9425.

[43] BUCK, U., and SCHMIDT, B., 1993, *J. chem. Phys.*, **98**, 9410.

[44] BUCK, U., 1994, *J. Phys. Chem.*, **98**, 5190.

[45] BUCK, U., and SCHMIDT, B., 1994, *J. chem. Phys.*, **101**, 6365.

[46] BUCK, U., 1995, *Adv. at. molec. opt. Phys.*, **35**, 121.

[47] HUISKEN, F., TARAKANOVA, E. G., VIGASIN, A. A., and YUKHNEVICH, G. V., 1995, *Chem. Phys. Lett.*, **245**, 319.

[48] HUISKEN, F., KALOUDIS, M., KULCKE, A., LAUSH, C., and LISY, J. M., 1995, *J. chem. Phys.*, **103**, 5366.

[49] BUCK, U., KROHNE, R., and SIEBERS, J., 1992, *Nuclear Physics Concepts in the Study of Atomic Cluster Physics*, Lecture Notes in Physics, Vol. 404, edited by R. Schmidt, H. O. Lutz and R. Dreizler (Berlin: Springer), p. 178.

[50] BUCK, U., KROHNE, R., and SIEBERS, J., 1993, *Z. Phys. D*, **26**, 169.

[51] BUCK, U., and KROHNE, R., 1994, *Phys. Rev. Lett.*, **73**, 947.

[52] BUCK, U., ETTISCHER, I., and SCHULZ, S., 1995, *Z. phys. Chem.*, **188**, 91.

[53] BUCHENAU, H., TOENNIES, J. P., and NORTHBY, J. A., 1991, *J. chem. Phys.*, **95**, 8134.

[54] BUCK, U., and WINTER, M., 1994, *Z. Phys. D*, **31**, 291.

[55] CHÂTELET, M., DE MARTINO, A., PETTERSON, J., PRADÈRE, F., and VACH, H., 1992, *Chem. Phys. Lett.*, **196**, 563.

[56] VACH, H., DE MARTINO, A., BENSLIMANE, M., CHÂTELET, M., and PRADÈRE, F., 1994, *J. chem. Phys.*, **100**, 8526.

[57] Benslimane, M., Châtelet, M., de Martino, A., Pradère, F., and Vach, H., 1995, *Chem. Phys. Lett.*, 237, 323.

[58] Gspann, J., and Krieg, G., 1974, *J. Chem. Phys.*, **61**, 4037.

[59] Cleveland, C. L., and Landman, U., 1992, *Science*, **257**, 355.

[60] Even, U., Schek, I., and Jortner, J., 1993, *Chem. Phys. Lett.*, **202**, 303.

[61] Schek, I., Raz, T., Levine, R. D., and Jortner, J., 1994, *J. chem. Phys.*, **101**, 8596.

[62] Raz, T., Schek, I., Ben-Nun, M., Even, U., Jortner, J., and Levine, R. D., 1994, *J. chem. Phys.*, **101**, 8606.

[63] Raz, T., and Levine, R. D., 1994, *J. phys. Chem.*, **99**, 7495.

[64] Raz, T., and Levine, R. D., 1995, *Chem. Phys. Lett.*, **246**, 405.

[65] Wren, D. J., and Menzinger, M., 1982, *Chem. Phys.*, **66**, 85.

[66] Nieman, J., and Naaman, R., 1984, *Chem. Phys.*, **90**, 407.

[67] Visticot, J. P., Mestdagh, J. M., Alcaraz, C., Cuvellier, J., and Berlande, J., 1988, *J. chem. Phys.*, **88**, 3081.

[68] Cuvellier, J., Mestdagh, J. M., Meynadier, P., de Pujo, P., Sublemontier, O., Visticot, J. P., Berlande, J., Bell, A. J., and Frey, J. G., 1991, *Chem. Phys.Lett.*, **176**, 325.

[69] Nieman, J., Shwartz, J., and Naaman, R., 1986, *Z. Phys. D*, **1**, 231.

[70] Nieman, J., and Naaman, R., 1986, *J. chem. Phys.*, **84**, 3825.

[71] Naaman, R., 1988, *Adv. chem. Phys.*, **70**, 181.

[72] Rudich, Y., Hurwitz, Y., Lifson, S., and Naaman, R., 1991, *J. Am. chem. Soc.*, **113**, 7077.

[73] Rudich, Y., Hurwitz, Y., Lifson, S., and Naaman, R., 1993, *J. chem. Phys.*, **98**, 2936.

[74] Hurwitz, Y., Rudich, Y., Naaman, R., and Gerber, R. B., 1993, *J. chem. Phys.*, **98**, 2941.

[75] Rudich, Y., Hurwitz, Y., Frost, G. J., Vaida, V., and Naaman, R., 1993, *J. chem. Phys.*, **99**, 4500.

[76] Hurwitz, Y., Rudich, Y., and Naaman, R., 1993, *Chem. Phys. Lett.*, **215**, 674.

[77] Hurwitz, Y., Rudich, Y., and Naaman, R., 1994, *Isr. J. Chem.*, **34**, 59.

[78] Hurwitz, Y., and Naaman, R., 1995, *J. chem. Phys.*, **102**, 1941.

[79] Kappes, M., and Leutwyler, S., 1988, *Atomic and Molecular Beam Methods*, edited by G. Scoles (Oxford University Press), part 1. 15.

[80] Italian Physical Society, 1990, *The Chemical Physics of Atomic and Molecular Clusters*, Proceedings of the International School of Physics 'Enrico Fermi'—Course CVII, edited by G. Scoles (Amsterdam: North-Holland).

[81] Campargue, R., 1984, *J. phys. Chem.*, **88**, 4466.

[82] Miller, D. R., 1988, *Atomic and Molecular Beam Methods*, edited by G. Scoles (Oxford University Press), part 1. 2.

[83] Hagena, O. F., 1981, *Surf. Sci.*, **106**, 101.

[84] Hagena, O. F., 1991, *Rev. Scient. Instrum.*, **63**, 2374.

[85] Hagena, O. F., 1987, *Z. Phys. D*, **4**, 291.

[86] Torchet, G., Farges, J., de Feraudy, M. F., and Raoult, B., 1990, *The Chemical Physics of Atomic and Molecular Clusters*, Proceedings of the International School of Physics 'Enrico Fermi'—Course CVII, edited by G. Scoles (Amsterdam: North-Holland), pp. 513–542.

[87] Farges, J., de Feraudy, M. F., Raoult, B., and Torchet, G., 1986, *J. chem. Phys.*, **84**, 3491.

[88] Torchet, G., Bouchier, H., Farges, J., de Feraudy, M. F., and Raoult, R., 1984, *J. chem. Phys.*, **81**, 2137.

[89] Torchet, G., de Feraudy, M. F., and Raoult, B., 1995, *J. chem. Phys.*, **103**, 3074.

[90] Bell, A. J., Mestdagh, J. M., Berlande, J., Biquard, X., Cuvellier, J., Lallement, A., Meynadier, P., Sublemontier, O., and Visticot, J. P., 1993, *J. Phys. D*, **26**, 994.

[91] Gspann, J., and Vollmar, H., 1974, *Rarefied Gas Dynamics*, edited by K. Karamcheti (New York: Academic Press), p. 261.

[92] Buck, U., and Meyer, H., 1984, *Phys. Rev. Lett.*, **52**, 109.

[93] Buck, U., and Meyer, H., 1985, *Surf. Sci.*, **156**, 275.

[94] Buck, U., 1990, *The Chemical Physics of Atomic and Molecular Clusters*, Proceedings of the Internaitonal School of Physics 'Enrico Fermi'—Course CVII, edited by G. Scoles (Amsterdam: North-Holland), pp. 543–577.

[95] Buck, U., and Krohne, R., 1996, *J. chem. Phys.*, **105**, 5408.

[96] LEWERENZ , M., SCHILLING , B., and TOENNIES , J. P., 1993, *Chem. Phys. Lett.*, **206**, 381.

[97] CUVELLIER , J., MEYNADIER , P., DE PUJO, P., SUBLEMONTIER , O., VISTICOT , J. P., BERLANDE , J., LALLEMENT , A., and MESTDAGH , J. M., 1991, *Z. Phys.* D, **21**, 265.

[98] DE MARTINO , A., BENSLIMANE , M., CHÂTELET , M., CROZES, C., PRADÈRE, F., and VACH, H., 1993, *Z. Phys.* D, **27**, 185.

[99] FARGES, J., DE FERAUDY , M. F., RAOULT , B., and TORCHET , G., 1988, *Adv. chem. Phys.*, **70**, 45.

[100] BARTELL , L. S., 1986, *Chem. Rec.*, **86**, 491.

[101] FARGES, J., RAOULT , R., and TORCHET , G., 1973, *J. chem. Phys.*, **59**, 3454.

[102] KIM, S. S., and STEIN, G. D., 1982, *J. Colloid Interface Sci.*, **87**, 180.

[103] FARGES, J., DE FERAUDY , M. F., RAOULT , R., and TORCHET , G., 1983, *J. chem. Phys.*, **78**, 5067.

[104] LEE, J. W., and STGEIN, G. D., 1985, *Surf. Sci.*, **156**, 112.

[105] RAOULT , B., FARGES, J., DE FERAUDY , M. F., and TORCHET , G., 1989, *Phil. Mag.* B, **60**, 881.

[106] VAN DE WAAL , B. W., 1996, *J. Crystal Growth*, **158**, 153.

[107] FARGES, J., DE FERAUDY , M. F., RAOULT , B., and TORCHET , G., 1984, *Ber. Bunsenges. phys. Chem.*, **88**, 211.

[108] TORCHET , G., FARGES, J., DE FERAUDY , M. F., and RAOULT , B., 1989, *Annls. Phys.* (*Paris*), **14**, 245.

[109] FARGES, J., DE FERAUDY , M. F., RAOULT , B., and TORCHET , G., 1985, *Surf. Sci.*, **156**, 444.

[110] TORCHET , G., DE FERAUDY , M. F., RAOULT , B., FARGES, J., FUCHS, A. H., and PAWLEY , G. S., 1990, *J. chem. Phys.*, **92**, 6768.

[111] BÉNIÈRE, F. M., BOUTIN, A., SIMON , J. M., FUCHS, A. H., DE FERAUDY , M. F., and TORCHET , G., 1993, *J. phys. Chem.*, **97**, 10472.

[112] TORCHET , G., SCHWARTZ , P., FARGES, J., DE FERAUDY , M. F., and RAOULT , B., 1983, *J. chem. Phys.*, **79**, 6196.

[113] BARTELL , L. S., HARSANYI, L., and VALENTE , E. J., 1989, *J. phys. Chem.*, **93**, 6201.

[114] BARTELL , L. S., and DIBBLE, T. S., 1990, *J. Am. chem. Soc.*, **112**, 890.

[115] BARTELL , L. S., and DIBBLE, T. S., 1991, *J. phys. Chem.*, **95**, 1159.

[116] BARTELL , L. S., 1995, *J. phys. Chem.*, **99**, 1080.

[117] HUANG , J., LU, W., and BARTELL , L. S., 1996, *J. phys. Chem.*, **100**, 14276.

[118] BARTELL , L. S., 1996, *J. phys. Chem.*, **100**, 8197.

[119] FARGES, J., DE FERAUDY , M. F., RAOULT , B., and TORCHET , G., 1981, *Surf. Sci.*, **106**, 95.

[120] HARTMANN , M., MILLER , R. E., TOENNIES , J. P., and VILESOV , A., 1995, *Phys. Rev. Lett.*, **75**, 1566.

[121] GSPANN , J., 1982, *Physics of Electronic and Atomic Collisions*, edited by S. Datz (Amsterdam : North-Holland), pp. 43–45.

[122] KLOTS, C. E., 1985, *J. chem. Phys.*, **83**, 5854.

[123] KLOTS, C. E., 1987, *Z. Phys.* D, **5**, 83.

[124] KLOTS, C. E., 1987, *Nature*, **327**, 222.

[125] KLOTS, C. E., 1988, *J. phys. Chem.*, **92**, 5864.

[126] KLOTS, C. E., 1991, *Z. Phys.* D, **20**, 105.

[127] KLOTS, C. E., 1991, *Z. Phys.* D, **21**, 335.

[128] NÄHER, U., and HANSEN , K., 1994, *J. chem. Phys.*, **101**, 5367.

[129] DUMONT , R. S., JAIN, S., and BASILE, A. G., 1995, *J. chem. Phys.*, **102**, 4227.

[130] BARTELL , L. S., and FRENCH , R. J., 1983, *J. chem. Phys.*, **79**, 2683.

[131] BARTELL , L. S., and French, R. J., 1989, *Rev. scient. Instrum.*, **60**, 1223.

[132] GOUGH , T. E., MENGEL , M., ROWNTREE , P. A., and SCOLES, G., 1985, *J. chem. Phys.*, **83**, 4958.

[133] SCHEIDEMANN , A., SCHILLING , B., and TOENNIES , J. P., 1990, *Physica* B, **165**, 135.

[134] HUISKEN , F., and STEMMLER , M., 1993, *J. chem. Phys.*, **98**, 7680.

[135] SCHULZ , C. P., HAUGSTÄTTER , R., TITTES, H. U., and HERTEL , I. V., 1986, *Phys. Rev. Lett.*, **57**, 1703.

[136] CAMPBELL , E. E. B., SCHMIDT , H., and HERTEL , I. V., 1988, *Adv. chem. Phys.*, **72**, 37.

[137] DEL MISTRO, G., and STACE, A. J., 1992, *Chem. Phys. Lett.*, **196**, 67.

[138] DE PUJO, P., MESTDAGH , J. M., VISTICOT , J. P., CUVELLIER , J., MEYNADIER , P., SUBLEMONTIER , O., LALLEMENT , A., and BERLANDE , J., 1993, *Z. Phys.* D, **25**, 357.

[139] GAIGEOT, M. P., DE PUJO, P., BRENNER, V., and MILLIÉ, P., 1997, *J. chem. Phys.* (submitted).

[140] LALLEMENT, A., MESTDAGH, J. M., MEYNADIER, P., DE PUJO, P., SUBLEMONTIER, O., VISTICOT, J. P., BERLANDE, J., BIQUARD, X., CUVELLIER, J., and HICKMAN, C. G., 1993, *J. chem. Phys.*, **99**, 8705.

[141] CUVELLIER, J., and BINET, A., 1988, *Rev. Phys. Appl.*, **23**, 91.

[142] BIQUARD, X., SUBLEMONTIER, O., VISTICOT, J. P., MESTDAGH, J. M., MEYNADIER, P., GAVEAU, M. A., and BERLANDE, J., 1994, *Z. Phys. D*, **30**, 45.

[143] ALLOUCHE, A. R., AUBERT-FRÉCON, M., NICOLAS, G., and SPIEGELMANN, F., 1995, *Chem. Phys.*, **200**, 63.

[144] BIQUARD, X., SUBLEMONTIER, O., BERLANDE, J., GAVEAU, M. A., MESTDAGH, J. M., and VISTICOT, J. P., 1995, *J. chem. Phys.*, **103**, 957.

[145] LEUTWYLER, S., and JORTNER, J., 1987, *J. phys. Chem.*, **91**, 5558.

[146] SCHMIDT, M., MONS, M., and LE CALVÉ, J., 1991, *Chem. Phys. Lett.*, **177**, 371.

[147] SCHMIDT, M., MONS, M., and LE CALVÉ, J., 1992, *J. phys. Chem.*, **96**, 2404.

[148] GUILLAUME, C., MONS, M., LE CALVÉ, J., and DIMICOLI, I., 1993, *J. phys. Chem.*, **97**, 5193.

[149] SCHMIDT, M., LE CALVÉ, J., and MONS, M., 1993, *J. chem. Phys.*, **98**, 6102.

[150] GUILLAUME, C., LE CALVÉ, J., DIMICOLI, I., and MONS, M., 1995, *J. Chim. phys.*, **92**, 334.

[151] TOPP, M. R., 1995, *J. Chim. phys.*, **92**, 310.

[152] GU, X. J., LEVANDIER, D. J., ZHANG, B., SCOLES, G., and ZHUANG, D., 1990, *J. chem. Phys.*, **93**, 4898.

[153] CELII, F. G., and JANDA, K. C., 1988, *Z. Phys. D*, **10**, 337.

[154] LEVANDIER, D. J., GOYAL, S., MCCOMBIE, J., PATE, B., and SCOLES, G., 1990, *J. chem. Soc.*, *Faraday Trans.*, **86**, 2361.

[155] PERERA, L., and AMAR, F. G., 1990, *J. chem. Phys.*, **93**, 4884.

[156] VISTICOT, J. P., BERLANDE, J., CUVELLIER, J., LALLEMENT, A., MESTDAGH, J. M., MEYNADIER, P., DE PUJO, P., and SUBLEMONTIER, O., 1992, *Chem. Phys. Lett.*, **191**, 107.

[157] VISTICOT, J. P., DE PUJO, P., MESTDAGH, J. M., LALLEMENT, A., BERLANDE, J., SUBLEMONTIER, O., MEYNADIER, P., and CUVELLIER, J., 1994, *J. chem. Phys.*, **100**, 158.

[158] LENGEN, M., JOPPIEN, M., VON PIETROWSKI, R., and MÖLLER, T., 1994, *Chem. Phys. Lett.*, **229**, 362.

[159] GOYAL, S., SCHUTT, D. L., and SCOLES, G., 1995, *J. chem. Phys.*, **102**, 2302.

[160] HARTMANN, M., MILLER, R. E., TOENNIES, J. P., and VILESOV, A., 1995, *Phys. Rev. Lett.*, **75**, 1566.

[161] SCHILLING, B., GAVEAU, M. A., SUBLEMONTIER, O., MESTDAGH, J. M., VISTICOT, J. P., BIQUARD, X., and BERLANDE, J., 1994, *J. chem. Phys.*, **101**, 5772.

[162] KRYLOV, A. I., GERBER, R. B., GAVEAU, M. A., MESTDAGH, J. M., SCHILLING, B., and VISTICOT, J. P., 1996, *J. chem. Phys.*, **104**, 3651.

[163] JUNGWIRTH, P., and GERBER, R. B., 1996, *J. chem. Phys.*, **104**, 5803.

[164] KUNZ, H., MCCAFFREY, J. G., SCHRIEVER, R., and SCHWENTNER, N., 1991, *J. chem. Phys.*, **94**, 1039.

[165] MCCAFFREY, J. G., KUNZ, H., and SCHWENTNER, N., 1992, *J. chem. Phys.*, **96**, 2825.

[166] MCCAFFREY, J. G., KUNZ, H., and SCHWENTNER, N., 1992, *J. chem. Phys.*, **96**, 155.

[167] GUTMANN, M., WILLBERG, D. M., and ZEWAIL, A. H., 1992, *J. chem. Phys.*, **97**, 8048.

[168] POTTER, E. D., LIU, Q., and ZEWAIL, A. H., 1992, *Chem. Phys. Lett.*, **200**, 605.

[169] LIU, Q., WANG, J. K., and ZEWAIL, A. H., 1993, *Nature*, **364**, 427.

[170] LIENAU, C., WILLIAMSON, J. C., and ZEWAIL, A. H., 1993, *Chem. Phys. Lett.*, **213**, 289.

[171] ZADOYAN, R., and APKARIAN, V. A., 1993, *Chem. Phys. Lett.*, **206**, 475.

[172] ZADOYAN, R., LI, Z., MARTENS, C. C., and APKARIAN, V. A., 1994, *Chem. Phys. Lett.*, **218**, 504.

[173] DEDONDER-LARDEUX, C., BERDAH, M., JOUVET, C., MARTRENCHARD-BARRA, S., MESTDAGH, J. M., SOLGADI, D., and VISTICOT, J. P., 1996, *J. chem. Phys.*, **104**, 2740.

[174] HARRIS, A. L., BROWN, J. K., and HARRIS, C. B., 1988, *A. Rev. chem. Phys.*, **39**, 341.

[175] ALIMI, R., GERBER, R. B., and APKARIAN, V. A., 1990, *J. chem. Phys.*, **92**, 1551.

[176] ALIMI, R., APKARIAN, V. A., and GERBER, R. B., 1993, *J. chem. Phys.*, **98**, 331.

[177] KRYLOV, A. I., GERBER, R. B., and APKARIAN, V. A., 1994, *Chem. Phys.*, **189**, 261.

[178] BEN-NUN, M., LEVINE, R. D., JONAS, D. M., and FLEMING, G. R., 1995, *Chem. Phys. Lett.*, **245**, 629.

[179] LIU, LI, and GUO, HUA, 1996, *J. chem. Phys.*, **104**, 528.
[180] SCHRÖDER, H., and GABRIEL, H., 1996, *J. chem. Phys.*, **104**, 587.
[181] STERLING, M., ZADOYAN, R., and APKARIAN, V. A., 1996, *J. chem. Phys.*, **104**, 6497.
[182] MESTDAGH, J. M., BERDAH, M., DEDONDER-LARDEUX, C., JOUVET, C., MARTRENCHARD-BARRA, S., SOLGADI, D., and VISTICOT, J. P., 1997, *J. chem. Phys.* (submitted).
[183] LEVANDIER, D. J., MCCOMBIE, J., PURSEL, R., and SCOLES, G., 1987, *J. chem. Phys.*, **86**, 7239.
[184] LEVANDIER, D. J., MENGEL, M., PURSEL, R., MCCOMBIE, J., and SCOLES, G., 1988, *Z. Phys.* D, **10**, 337.
[185] STIENKEMEIER, F., HIGGINS, J., ERNST, W. E., and SCOLES, G., 1995, *Phys. Rev. Lett.*, **74**, 3592.
[186] STIENKEMEIER, F., ERNST, W. E., HIGGINS, J., and SCOLES, G., 1995, *J. chem. Phys.*, **102**, 615.
[187] LEWERENZ, M., SCHILLING, B., and TOENNIES, J. P., 1995, *J. chem. Phys.*, **102**, 8191.
[188] SCHMIDT, B., and GERBER, R. B., 1994, *Phys. Rev. Lett.*, **72**, 2490.
[189] SCHMIDT, B., and GERBER, R. B., 1994, *J. chem. Phys.*, **101**, 343.
[190] GÉE, C., GAVEAU, M. A., MESTDAGH, J. M., OSBORNE, M., SUBLEMONTIER, O., and VISTICOT, J. P., 1996, *J. phys. Chem.*, **100**, 13421.
[191] LALLEMENT, A., CUVELLIER, J., MESTDAGH, J. M., MEYNADIER, P., DE PUJO, P., SUBLEMONTIER, O., VISTICOT, J. P., BERLANDE, J., and BIQUARD, X., 1992, *Chem. Phys. Lett.*, **189**, 182.
[192] HU, X., and MARTENS, C. C., 1993, *J. chem. Phys.*, **99**, 9532.
[193] GAVEAU, M. A., SCHILLING, B., GÉE, C., SUBLEMONTIER, O., VISTICOT, J. P., MESTDAGH, J. M., and BERLANDE, J., 1995, *Chem. Phys. Lett.*, **246**, 307.
[194] BIQUARD, X., SUBLEMONTIER, O., BERLANDE, J., GAVEAU, M. A., MESTDAGH, J. M., SCHILLING, B., and VISTICOT, J. P., 1995, *J. Chim. phys.*, **92**, 264.
[195] LALLEMENT, A., BELL, A. J., BERLANDE, J., CUVELLIER, J., MESTDAGH, J. M., MEYNADIER, P., SUBLEMONTIER, O., and VISTICOT, J. P., 1993, *Chem. Phys. Lett.*, **204**, 440.
[196] KELLY, F. M., and MATHUR, M. S., 1972, *Can. J. Phys.*, **55**, 83.
[197] OSBORNE, M. A., GAVEAU, M. A., GÉE, C., SUBLEMONTIER, O., MESTDAGH, J. M., and VISTICOT, J. P., 1997, *J. chem. Phys.*, **106** (in press).
[198] BILLY, N., GIRARD, B., GOUÉDARD, G., and VIGUÉ, J., 1990, *Laser Chem.*, **10**, 319.
[199] MESTDAGH, J. M., VISTICOT, J. P., and SUITS, A. G., 1995, *The Chemical Dynamics and Kinetics of Small Radicals*, edited by K. Liu and A. Wagner (Singapore: World Scientific), pp. 668–729.
[200] JONAH, C. D., and ZARE, R. N., 1971, *Chem. Phys. Lett.*, **9**.
[201] MENZINGER, M., 1985, *Gas-Phase Chemiluminescence and Chemi-Ionization*, edited by A. Fontijn (Paris: Elsevier), pp. 25–66.
[202] BEN-NUN, M., and LEVINE, R. D., 1992, *J. chem. Phys.*, **97**, 8341.
[203] BEN-NUN, M., and LEVINE, R. D., 1992, *J. phys. Chem.*, **97**, 2334.
[204] GÉE, C., GAVEAU, M. A., SUBLEMONTIER, O., MESTDAGH, J. M., and VISTICOT, J. P., 1997, *J. phys. Chem.* (submitted).
[205] CHEVALEYRE, J., 1996, private communication.